

Characterization of long non coding RNA LINC1 in Colorectal Cancer

by

Anna-Maria Pehserl, BSc

to be awarded the academic degree

Master of science

Masterstudium Biochemie und Molekulare Biomedizin

at the

Technical University of Graz

supervisor

Assoz.-Prof. Priv.-Doz. Mag.rer.nat. Dr.med.univ. Martin Pichler

Division of Clinical Oncology,

Department of Internal Medicine,

Medical University of Graz

Graz, 2017

EIDENSTÄTTLICHE ERKLÄRUNG

Ich erkläre an Eides statt, dass ich die vorliegende Arbeit selbständig verfasst, andere als die angegebenen Quellen/Hilfsmittel nicht benutzt und die den benutzten Quellen wörtlich und inhaltlich entnommenen Stellen als solche kenntlich gemacht habe. Das in TUGRAZonline hochgeladenen Textdokument ist mit der vorliegenden Masterarbeit identisch.

Datum

Unterschrift

Acknowledgment

First of all I would like to thank my supervisor Martin Pichler for giving me the opportunity to work on this interesting topic. I am deeply grateful for his encouragement, guidance and support during my Master's thesis in his lab.

I especially want to thank Verena Stiegelbauer for her kind assistance during my whole work.

Furthermore, I would like to thank all my team colleagues Verena, Daniela, Steffi, Margit, JB, Lisa, Andreas and Johannes for their help, great support and friendship.

I also want to thank the other lab members Bianca, Moni, Bettina, Angela, Irina, Verena, Theresa, Stefanie, and Jaqui.

Thanks to all my friends who supported me during this time.

Last but not least my family. I am deeply grateful for the support I received from my family especially my parents.

Abbreviations

5-FU	5-fluorouracil
APC	adenomatous polyposis coli
BRAF	v-raf murine sarcoma viral oncogene homolog B
CCAT1	colon cancer associated transcript 1
cDNA	complementary DNA
CIMP	CpG island methylator phenotype
CIN	chromosomal instability
CRC	colorectal cancer
DNA	Deoxyribonucleic acid
EGF	epidermal growth factor
eIF4A3	eukaryotic translation initiation factor 4A3
EtOH	Ethanol
FAP	family adenomatous polyposis
FBS	foetal bovine serum
FGF	fibroblast growth factor
HE	hematoxilin-eosin
HNPCC	Hereditary nonpolyposis colon cancer
HOTAIR	HOX transcript antisense RNA
IBD	inflammatory bowel disease
IGF2	insulin-like growth factor II
IgG2	Immunglobulin G2

KRAS	Kristen rat sarcoma viral oncogene homolog
lincRNA	long intergenic RNA
lncRNA	long non-coding RNA
LOH	loss of heterozygosity
LS	Lynch syndrome
MALAT-1	metastasis associated lung adenocarcinoma transcript 1
mCRC	metastatic CRC
miRNA	micro RNA
MMR	mismatch repair
mRNA	messenger RNA
MSI	microsatellite instability
ncRNA	non-coding RNA
NEAT1	nuclear-enriched abundant transcript 1
ORF	open reading frame
PBS	phosphate-buffered saline
PCR	polymerase chain reaction
PI	propidium iodide
PRC2	polycomb repressive complex 2
RB	retinoblastoma protein
RIPA	Radioimmunoprecipitation assay
RNA	Ribonucleic acid
RNAi	RNA interfering
RT-qPCR	real-time quantitative PCR

siRNA	small interfering RNA
TBS	Tris buffered saline
TBS-T	Tris buffered saline with Tween 2.0
TGF-alpha	transforming growth factor alpha
TNM	tumor node metastasis
UTR	untranslated region
Xic	X-inactivation center
XIST/Xist	X-inactive-specific transcript

Abstract

Colorectal cancer (CRC) is one of the leading causes of cancer related death worldwide. Despite substantial progress in understanding the molecular mechanisms and treatment of CRC in the last years, the overall survival rate of CRC patients has not improved significantly. Therefore, it is of great importance to find novel molecular factors that can predict the progression and prognosis in colorectal cancer patients as well as to discover new molecules that can act as therapeutic targets.

In recent years long non coding RNAs (lncRNAs) have moved into the focus of research. They play a pivotal role in the regulation of various cell processes and have been associated with the development and progression of different cancer types. This knowledge makes them suitable as biomarkers for cancer diagnosis and prognosis.

In this thesis we investigated the biological function of a novel lncRNA *LINC1* in CRC cell lines *in vitro* and *in vivo*. For this purpose, we performed loss of function experiments in a panel of CRC cell lines to evaluate the impact of *LINC1* on proliferation, migration, apoptosis, cell cycle, stemness *in vitro* and *in vivo*.

Zusammenfassung

Kolorektalkarzinom (CRC) ist eine der führenden, tödlichen Ursachen von Krebs weltweit. Trotz erheblicher Fortschritte im Bereich der molekularen Mechanismen und in der Behandlung von CRC hat sich die Überlebensrate von Patienten in den letzten Jahren nicht wesentlich verbessert. Daher ist es von großem Interesse, neue molekulare Faktoren zu finden, welche die Progression und Prognose bei Dickdarmkrebspatienten verbessern und weitere Moleküle zu finde welche als therapeutisches Ziel eingesetzt werden können. Lange nicht kodierende RNAs (lncRNAs) sind in den letzten Jahren in den Fokus der Forschung gerückt. Sie spielen eine zentrale Rolle bei der Regulierung verschiedener Zellprozesse und werden mit dem Fortschreiten und der Entwicklung verschiedener Krebsarten assoziiert. Dadurch machen sich lncRNAs zu einem geeigneten Biomarker für die Krebs Diagnose und Prognose. In dieser Arbeit untersuchen wir die biologische Funktion einer neuartigen lncRNA LINC1 in CRC Zelllinien *in vitro* und *in vivo*. Der Effekt von LINC1 knockdown wurde auf Proliferation, Migration, Apoptose, Zellzyklus und Stammzellfähigkeit hin untersucht.

List of figures

Figure 1: Relative expression levels in CRC cell lines.....	32
Figure 2: Knock down of <i>LINC1</i> in CRC cell lines.....	33
Figure 3: Colony forming unit assay	35
Figure 4: Soft Agar Assay.	36
Figure 5: WST-1 Proliferation assay.....	37
Figure 6: Tumorsphere formation assay.....	38
Figure 7: Wound healing scratch assay.....	39
Figure 8: Apoptosis assay.	40
Figure 9: Western Blot PARP detection in <i>LINC1</i> silenced CRC cell lines.	41
Figure 10: Cell cycle analysis.	42
Figure 11: Xenograft mouse model.	43
Figure 12: Xenograft mouse model maximal diameter tumor tissue.	44
Figure 13: Representative picture of HE stained FFPE xenograft tumor tissues.	45

List of tables

Table 1: Genomic DNA elimination.....	25
Table 2: Mastermix for cDNA synthesis.....	26
Table 3: cDNA synthesis: cycling program.....	26
Table 4: Mastermix for qRT-PCR.....	27
Table 5: qRT-PCR program.....	27
Table 6: Primer sequences for qRT-PCR.....	28

Table of Contents

Acknowledgment.....	I
Abbreviations.....	II
Abstract	V
Zusammenfassung.....	VI
List of figures	VII
List of tables	VIII
1 Introduction.....	11
1.1 Epidemiology and risk factors.....	11
1.2 Mechanisms of carcinogenesis	11
1.3 Treatment regimes	12
1.4 Chemotherapeutic drugs	12
1.5 EGFR targeted therapy.....	13
1.6 Long non coding RNA.....	14
1.7 LncRNAs involved in the invasion, metastasis, early diagnosis and prognosis of CRC	14
1.8 Epigenetic modifications.....	16
1.9 LINC1.....	17
Aim of the study	18
2 Material and Methods.....	19
2.1 Cell culture.....	19
2.1.1 Cultivation of cell lines.....	19
2.1.2 Trypsinations of cells.....	19
2.1.3 siRNA transfection.....	20
2.2 Cellulare assays.....	21
2.2.1 WST-1 proliferation assay	21
2.2.2 Wound healing scratch assay.....	21
2.2.3 Clonogenic assay.....	22
2.2.4 Soft agar colony formation assay.....	22
2.2.5 Tumorsphere formation assay	22
2.2.6 Apoptosis assay.....	23
2.2.7 Cell Cycle assay.....	23
2.3 Gene expression analysis	24
2.3.1 RNA Isolation.....	24
2.3.2 TURBO Dnase Treatment.....	IX

2.3.3	Reverse Transcription cDNA synthesis.....	25
2.3.4	Quantitative real time PCR (qRT-PCR).....	26
2.3.5	Calculation of relative gene expression	28
2.4	Western Blot analysis.....	28
2.4.1	Protein Isolation	28
2.4.2	SDS PAGE and wet transfer	29
2.4.3	Detection of protein expression	29
2.4.4	Detection of β -actin protein expression.....	30
2.4.5	Relative quantification of protein expression.....	30
2.4.6	Xenograft mouse model.....	30
2.5	Statistical analysis	31
3	Results.....	32
3.1	LINC1 Expression analysis in CRC cell lines.....	32
3.2	Establishing knock down technique for LINC1.....	33
3.3	Colony forming unit assay	34
3.4	Soft Agar Assay	36
3.5	WST-1 Proliferation Assay	37
3.6	Tumorsphere formation assay	38
3.7	Wound healing scratch assay.....	39
3.8	Apoptosis Assay Caspase 3/7.....	40
3.9	Western Blot PARP	41
3.10	Cell cycle analysis	41
3.11	Xenograft mouse model.....	42
4	Discussion.....	46
5	Conclusion and outlook	49
6	References.....	50

1 Introduction

1.1 Epidemiology and risk factors

Colorectal cancer (CRC) is among the leading causes of cancer related mortality worldwide. It is the third most common cancer diagnosed in men and females and represents the most frequent cancer of the digestive system. In 2016, about 63670 females and 70820 men were diagnosed with CRC (1). Sex, age, hereditary and personal history are independent risk factors for CRC. The incidence increases around the age of 40 years (2). In addition to age, also the personal history of CRC or inflammatory bowel disease (IBD) cannot be modified (3). The chronic inflammation found in IBD often produces atypical cell growth known as dysplasia. Despite dysplastic cells are not yet malignant, they have more chances of becoming anaplastic and developing into a tumor (4). Other risk factors can be reduced by implementing modest lifecycle changes in terms of dietary and physical activity habits (5). Another important risk factor is related to a sedentary lifestyle such as obesity (6). Moreover, smoking and alcohol consumption have also been shown to increase the chances of suffering from CRC by up to 10,8% due to the high content in carcinogenesis such as nicotine, the metabolites of which can easily reach the intestine and generate polyps (7, 8). About 75% of all new cases of CRC occur in people with no predisposition factors which are considered to be at average risk of CRC. Hereditary nonpolyposis colon cancer (HNPCC), also known as Lynch syndrome, accounts for about 5% of new cases of CRC each year and people with family adenomatous polyposis (FAP) for approximately 1% of new cases (2). Lifetime risk of developing CRC is double among those with first degree relative having CRC, and the risk increases 4-fold if the diagnosis is set before the age of 45 years (4).

1.2 Mechanisms of carcinogenesis

CRC can emerge from one or a combination of three different mechanisms, especially chromosomal instability (CIN), CpG island methylator phenotype (CIMP)

and microsatellite instability (MSI). The classical CIN pathway starts with the acquisition of mutations in the adenomatous polyposis coli (APC), ensured by the mutational activation of oncogene KRAS and the inactivation of the tumor suppressor gene, TP53 (9). The major player in CIN tumors are aneuploidy and loss of heterozygosity (LOH), which not only constitute most of the sporadic tumors (85%) but also involve familial adenomatous polyposis cases associated with germline mutation in the APC gene (10). The CIMP pathway is described by promotor hypermethylation of various tumor suppressor genes such as MGMT and MLH1. This hypermethylation often is associated with BRAF mutation and microsatellite instability (11). The MSI pathway affects the inactivation of genetic alteration in short repeated sequences. This activation is a hallmark condition in familial Lynch syndrome (LS) and occurs in CRC in DNA mismatch repair (MMR) genes (12).

1.3 Treatment regimes

In the past few years the survival rates of individuals with colorectal cancer have increased substantially, possibly as a result of early diagnosis and improved treatment. Despite significant information about risk factors exists, about 75% of diagnosis remain unclear in patients with no apparent risk factors other than older age (13). The 5 year survival rates after surgical resection for patients with localized disease has dramatically improved. However more than half of all patients diagnosed with CRC finally develop recurrence of their disease and metastasis (13, 14). For patients with metastatic CRC there have been several changes in treatment over the past years. For example, incorporation of new chemotherapeutic drugs, the introduction of novel targeting agents such as inhibitors of angiogenesis and epidermal growth factor receptor signaling which improved survival time of metastatic CRC (mCRC) patient (15).

1.4 Chemotherapeutic drugs

The antimetabolite 5-fluorouracil (5-FU) is the most studied drug in CRC (16). 5-FU is extensively used in the treatment of cancers including breast, CRC, head and neck (17, 18). However, the response rates for 5-FU based chemotherapy as a first line treatment for advanced CRC cancer are only 10-15% (19). 5-FU combined with new cytotoxic drugs such as oxaliplatin and irinotecan have improved the response rates to 40-50% (20, 21). Moreover, novel biological agents such as the monoclonal antibodies cetuximab and bevacizumab have shown additional benefits in patients with metastatic disease (22, 23).

1.5 EGFR targeted therapy

EGFR is a member of the ErbB family of the human epidermal factor receptors and is relevant in colorectal cancer because expression or up-regulation of the EGFR gene occurs in 60 to 80% of cases (24-26). The signalling pathway of EGFR controls cell proliferation, differentiation, migration, angiogenesis and apoptosis. All of which become deregulated in cancer cells (27). As a monomer EGFR is inactive. However, when bound by epidermal growth factor or transforming growth factor alpha (TGF-alpha), it forms homo or heterodimers with another member of the ErbB family of receptors. This dimerization triggers the intracellular tyrosine kinase region of EGFR, emerging in autophosphorylation and furthermore initiating a cascade of intracellular events (28). Therefore monoclonal antibodies that target EGFR can be effective as anticancer therapy. Cetuximab and Panitumumab are two monoclonal antibodies that target EGFR and have a clinical impact against CRC. Panitumumab is fully humanized IgG2 antibody and cetuximab a recombinant, chimeric, IgG1 monoclonal antibody. This different isotypes may be the decisive that these two antibodies differ in their mechanism of action (22). A resistance to anti-EGFR therapy in CRC is associated with molecular alterations of KRAS (29). Studies have shown that a high gene copy number of EGFR could be a potential marker for EGFR targeted therapy in CRC, as patients with low gene copy number are unlikely to respond to anti-EGFR agents (30, 31).

1.6 Long non coding RNA

RNAs that do not encode proteins are called non-coding RNAs (ncRNA) and those with a length more than 200 nucleotides are referred to as long non-coding RNAs (lncRNAs) (32). Long non coding RNAs are one of the most poorly understood, yet most common RNA species. Since they represent an extensive, large unexplored and functional component of the genome the study is of major relevance to the human biology and disease (33, 34). These non-coding RNAs have completely changed our understanding about the genetic code. The complexity of human physiology now cannot be exclusively defined by the expression of only 20000 protein-coding genes, but rather through interplay of the protein-coding genome and the non-coding genome (35). LncRNAs are roughly classified based on their position to protein-coding genes: intergenic (between genes), intragenic/intronic (within genes) and antisense (36).

1.7 LncRNAs involved in the invasion, metastasis, early diagnosis and prognosis of CRC

An increasing number of studies have shown that abnormal expression of lncRNAs may inhibit tumor suppressor genes or cancer-promoting genes in the development of CRC (37, 38). Furthermore, recent studies have demonstrated different and unique expression of lncRNA in CRC which could serve as new molecular markers in the tumor diagnosis and treatment (39).

HOTAIR

HOTAIR (HOX transcript antisense RNA is located on chromosome 12q13.13 and the first lncRNA found to demonstrate trans-transcriptional regulations function. Previous research has demonstrated that HOTAIR plays an essential role in various tumors including gastric cancer, breast cancer, cervical cancer and prostate cancer (40-43). High HOTAIR expression is correlated with a poor prognosis in CRC patients and it interacts with the polycomb repressive complex 2 (44). A decreasing

expression of HOTAIR has been indicated to inhibit the growth of human CRC cells (45). As it is only highly expressed in the primary tumors of CRC patients and found in the peripheral blood HOTAIR has potential as a prognostic factor (46).

CCAT

A recently discovered lncRNA is the colon cancer associated transcript 1 (CCAT1) which is located on chromosome 8p24.21 (47). Recent research has shown that CCAT1 is involved in colorectal carcinoma, gastric cancer and in esophageal squamous cell carcinoma (48, 49). The level of CCAT1 is significantly higher in the plasma of CRC patients compared with that of healthy controls (50, 51). Furthermore the CCAT1 overexpression is associated with CRC proliferation and invasiveness, lymph node metastasis, clinical stage and survival time of CRC (52-54).

MALAT-1

Metastasis associated lung adenocarcinoma transcript 1 (MALAT-1) is located on chromosome 11q13.1 and is involved in divers types of cancer such as breast cancer, lung cancer, pancreatic cancer, liver cancer and gastrointestinal cancer (55-57). MALAT-1 is upregulated in CRC and can promote cell proliferation, invasion and metastasis in CRC (58, 59). The high expression of MALAT-1 has been identified as a biomarker for poor prognosis in CRC (60) and the 3' end of MALAT-1 also is an important position in terms of invasion and metastasis in CRC (61).

H19

H19 is a 2.3kb lncRNA, constitutes a pair of imprinted genes together with the insulin-like growth factor-II gene (IGF2) and is located on chromosome 11q15.5 (62). Hypomethylation of H19 and IGF2 is involved in loss of imprinting of IGF2 in CRC (62) H19 expression demonstrated a link to a variety of cancers including breast cancer, gastric cancer and lung cancer (63). Overexpression of H19 is associated with tumor differentiation and tumor node metastasis (TNM) staging and also recruits the eukaryotic translation initiation factor 4A3 (eIF4A3) to stimulate CRC proliferation. In CRC patients, H19 is an independent predictor of overall survival and disease-free survival (64) H19 and its product miR-675 are upregulated in CRC. High levels of miR-675 have been demonstrated to reduce the expression of tumor suppressor

retinoblastoma protein (RB) through recognizing and binding the 3'end of its UTR (65).

lncRNA-p21

lncRNA-p21 is down regulated in CRC and is controlled by p53 to reduce cell viability (66). It reduces cancer cell survival and self-renewal capacity and promotes cancer cell glycolysis via inhibiting the β -catenin signal to inhibit CRC cells with stemness features from developing into mature cancer cells (67). lncRNA-p21 is also related to gastric cancer, hepatocellular carcinoma and to non-small cell lung cancer (68, 69).

NEAT 1

Nuclear-enriched abundant transcript 1 (NEAT1) is a nuclear-restricted lncRNA and has two isoforms, NEAT1_1 and NEAT1_2 (70). NEAT1 has been associated to be involved in gastric cancer, breast cancer and ovarian cancer (71) It is a possible biomarker for prognosis in CRC and the overexpression of NEAT1 in the whole blood and tissue of CRC patients is linked to tumor invasion, differentiation, metastasis and TNM staging (72).

1.8 Epigenetic modifications

lncRNAs play an important role in regulation of gene expression including modification of chromatin, controlling transcription and translation. Most of the antisense RNAs act in cis while other often act in trans for example lincRNAs. Therefore they can either function as positive or negative regulators of gene expression (73). lncRNAs interact with a variety of chromatin modification enzymes and also induce chromatin modification and DNA methylation (74, 75). They also participate in allele silencing and the maintenance of epigenetic modifications during embryonic development (76, 77). As a typical model for understanding epigenetic transcriptional regulation by lncRNA serves the X-inactivation center (Xic). X.inactivation by the X-inactive-specific transcript (XIST/Xist) in mammals is a common example. The Xist RNA binds directly to the polycomb repressive complex 2 (PRC2) which is the epigenetic complex responsible for silencing the whole chromosome (77). The lncRNA HOTAIR₁₆ can also bind to PRC2 and interact with

chromatin remodelling complexes to induce heterochromatin formation leading to a reduced target gene expression (38, 44).

1.9 LINC1

In this thesis, we worked with the novel lncRNA LINC00597. Throughout this study LINC00597 is referred to as intergenic non-coding RNA 1 (LINC1). The gene that encodes LINC1 is located on the reverse strand of chromosome 15q24.3 and only consist of 1 exon. Since LINC1 is an uncharacterized lncRNA yet, studies on the biochemical mechanisms and biological functions are still missing.

Aim of the study

Since lncRNAs might serve as potential predicting and prognostic factors and even as therapeutic targets themselves we aimed to examine the biological relevance of LINC1 in CRC. Previous investigations of the research group of Prof. Martin Pichler led to the hypothesis that LINC1 may play a functional role in colorectal cancer.

The following steps were taken to achieve these goals:

Characterization of the biological role of LINC1 silencing

- Evaluation of reproductive viability
- Performing *in vitro* proliferation assays
- Investigation of cellular anchorage –independent growth
- Cell cycle analysis
- Analysis of apoptotic activity
- *In vivo* confirmation of *in vitro* observations in nude mice

2 Material and Methods

2.1 Cell culture

2.1.1 Cultivation of cell lines

The human CRC cell lines HRT-18, SW480, DLD1 and HCT116, were purchased from American Type Culture Collection (Manassas, CA, USA) and their origin was proven by DNA identity STR-analysis. For HCT116 McCoy's 5A modified Medium (w/o L-Glutamine, 2,2g/L sodium bicarbonate) was used. HRT-18, SW480 and DLD1 cells were maintained in RPMI 1640 (GIBCO Lifetech, Vienna, Austria) containing 2mmol of L-glutamine. All growth media contained 10% foetal bovine serum (FBS) gold (Biochrome, Austria) and antibiotics (50 units per ml of penicillin, 50µg/ml of streptomycin). Cells were incubated in a 5% CO₂ humidified atmosphere at 37°C. The CRC cell lines HCT116, HRT18, SW480 and DLD1 were authenticated at the Cell bank of the Core Facility of the Medical University of Graz, Austria by performing a STR profiling analysis (Kit: Promega, PowerPlex 16HS System; Cat.No. DC2101, last date of testing: March 3rd 2016).

2.1.2 Trypsinations of cells

Adherent cells need to be detached from culture flasks before counting and seeding them again in the desired culture well or flask (Corning, Corning, NY). Detachment of cells was performed using trypsin/EDTA (Invitrogen, Carlsbad, CA). First, culture medium was removed and cells were washed with pre-warmed (37°C) Phosphate Buffered Saline (PBS; 4ml for 75cm² flasks, 2ml for 25cm² flasks or 1ml for 6 well plates, respectively). Afterwards, pre-warmed 1X trypsin/EDTA (2ml for 75cm² flasks, 1ml for 25cm² flasks or 0.5ml for 6 well plates, respectively) was added and incubated for 3-5 minutes until single cells are present (control under microscope). To stop the reaction, 3-fold volume of culture¹⁹ medium containing FBS was added.

Detached cells were resuspended in culture medium, collected in a 15ml falcon tube (Falcon ® Corning, Corning, NY) and centrifuged for 5 minutes at 800 rpm (rounds per minute). The supernatant was removed and the cell pellet was resuspended in 10 ml of fresh medium. Cell counting and determination of viability was done using a Biorad TC20 Cell Counter (Biorad, Hercules, CA). Therefore, 10 µl of cell suspension were mixed with 10 µl of trypan blue (Sigma) and were applied to a chamber of a Biorad Cell Counting slide. The appropriate amount of cell suspension was then transferred to a new tissue culture flask or well plate.

2.1.3 siRNA transfection

The cells were cultured in complete growth medium containing 10% FBS and 1% penicillin/streptomycin (50 units per ml of penicillin, 50µg/ml of streptomycin) at 37°C. To obtain silencing, HRT-18, SW480, DLD1 and HCT116 cells were trypsinized and transiently transfected with siRNAs targeting siRNA#1 (50nM, Hs_C15orf5_6) and siRNA#2 (50nM, Hs_C15orf5_8) (Qiagen, Hilde, Germany) as well as with a AllStars Negative Control (50nM, Qiagen, Hilde, Germany) and AllStars Cell Death Control (50nM, Qiagen, Hilde, Germany) using the fast forward procedure according to the HiPerfect Transfection Reagent (Qiagen) protocol. The cells were either transfected in 6 well plates or in 96 well plates using the HiPerfect Transfection Kit (Qiagen). For transfection in a 6 well plate (Corning, NY), containing $2,5 \times 10^5$ cells were seeded in a volume of 2.3 ml growth medium. A transfection mix containing 50 nM of respective siRNA, 10µl of HiPerfect Transfection Reagent and serum-free medium (total volume 100 µl) was prepared. The transfection mix was incubated for 10 minutes at room temperature and was then added to the cells. Cells were incubated under their normal growth conditions (37°C, 5% CO₂). RNA and protein isolation was performed after 48, 72 and 96 hours, respectively.

2.2 Cellulare assays

2.2.1 WST-1 proliferation assay

To examine whether altered *LINC1* silencing influences cellular growth rates of CRC cells, we applied the WST-1 proliferation assay (Roche Applied Science). After transfection, we measured the cellular growth rate at every 24 hours over a period of time of 96 hours. In more detail, after standard trypsinisation 3×10^3 CRC cells per well were seeded in a 96-well culture plate. After transfection with siRNA#1, siRNA#2, AllStars Negative Control (Qiagen) and AllStars Cell Death Control (Qiagen), cells were incubated in 200 μ l of normal growth medium for 96 h and the WST-1 proliferation reagent (Roche Applied Science) was added every 24 hours according to the manufacturer's recommendations. After 3 hours the colorimetric changes were measured using a SpectraMax Plus (Molecular Devices) at a wavelength of 450nm with a reference wavelength at 620 nm. The assay was performed in six technical replicates.

2.2.2 Wound healing scratch assay

To analysis cell migration a wound-healing assay was performed. After transient transfection of CRC cell lines HCT116, HRT-18 and SW480 at a density of 150×10^3 , cells were seeded in 24 well plates. After 24 hours of incubation, a scratch was made with a 100 μ l pipette tip to form a defined gap in the cell monolayer. After washing the cells with PBS, medium containing 10% FBS was added and cell migration toward the gap area was documented using a microscope at 10x magnification. The size of the gap at a selected position was measured using the cellSense Imaging software (Olympus, Hamburg, Germany) at the starting point of the experiment (0h= 0 hours), after 24 hours (24h) and up to 48 hours (48h). The ratio of the gap size at certain time points to the gap size at 0 h was calculated and replicates were averaged. The scratch assay was performed with 3 biological replicates.

2.2.3 Clonogenic assay

To evaluate reproductive viability after knock down, transfected cells (HCT116, HRT-18, SW480 and DLD1) were seeded into 6 well plates (200cells/well) in a volume of 2ml in standard growth medium. Cells were then cultured at 37°C and 5% CO₂ for up to 2 weeks. After colony formation, the colonies were stained with 0.05% crystal violet (Sigma) in 25% methanol and the number of colonies was counted using a dissecting microscope. The assay was performed with 6 technical replicates.

2.2.4 Soft agar colony formation assay

To measure anchorage - independent growth, 6 well plates were coated with 1 ml of 0.5 % agarose in culture medium. CRC cells (HCT116, HRT-18, SW480 and DLD1) at a density of 2×10^3 were then suspended in 0.35 % low gelling agarose in medium and overlaid on the coated plates. 1 ml of culture medium was added and fresh medium was added every week, once the agarose was solid. After approximately 6 weeks colony formation could be detected and colonies were stained with 0.005 % crystal violet solution (in PBS + 20 % EtOH) and then counted.

2.2.5 Tumorsphere formation assay

CRC cells HCT116, SW480 and DLD1 were transiently transfected and then harvested and resuspended in serum-free medium supplemented with 1 x B27 supplement, 20 ng/ml human epidermal growth factor (EGF), 10 ng/ml human basic fibroblast growth factor (FGF) and 300 IU Heparin. The cells were then seeded in ultra-low attachment 6 well plates at a density of 2×10^3 . After 10 – 16 days spheres were counted. Three technical replicates were made.

2.2.6 Apoptosis assay

Apoptosis in CRC cells HCT116, SW480 and DLD1 was examined using the Caspase-Glo 3/7 assay kits according to the manufacturer's instructions (Promega, Madison, WI). The cells were first seeded in triplicates in 96-well plates at a density of 3×10^3 and transfected with specific siRNAs against *LINC1* or respective control. For Caspase 3/7, after 48 and 96 hours cells were incubated, protected from light, with the caspase substrate for 30 minutes followed by measurements with a LUMIstar microtiter plate reader (BMG Labtech).

2.2.7 Cell Cycle assay

The CRC cell lines HCT116 and SW480 were transiently transfected and seeded in 6 well plates at a density of $2,5 \times 10^5$ for further analyses of cell cycle and apoptosis. Cells were detached from the culture dishes after 48h and 72h with Trypsin and washed with 5 ml PBS. After centrifugation at $800 \times g$ for 5 min at room temperature, cells were resuspended in 1 ml cold PBS. 3 ml of ice-cold 100 % EtOH was added dropwise to each sample under gentle vortexing. Samples were then incubated at 4 °C overnight. The cells were centrifuged at $800 \times g$ for 5 min and the EtOH was discarded. Cells were washed in 1 ml PBS (+ 0.2 % BSA) and pelleted. After 20 min at room temperature incubation of the dissolved cells with a hypotonic lysis solution containing 50 µg/mL propidium iodide (PI; Sigma, Vienna, Austria) and 100 µg/mL RNase (Fermentas, Thermo Fischer Scientific), cells were stored on ice in the dark for maximum one hour until flow cytometric measurement were performed. The analysis where done with Flow Cytometry (Thermo Fischer Scientific) which was performed according to the manufacturer's instructions. The Data was analyzed using the ModFit LT software (Verity software house, Topsham, ME, USA). The assay was performed with 3 biological replicates.

2.3 Gene expression analysis

2.3.1 RNA Isolation

Cells were cultured in well plates or tissues culture flask and after reaching 70-80% confluency cells were ready for RNA Isolation. Therefore, cells were washed with 1x PBS and afterwards 1 ml of TRIZOL reagent (Invitrogen, Carlsbad, CA) was directly added to the cells. Cells were transferred to a 2 ml Eppendorf tube (Eppendorf, Hamburg, Germany) and homogenized by passing through syringe and needle. Homogenized samples were incubated for 5 minutes at room temperature to permit the complete dissociation of nucleoprotein complexes.

For phase separation 100µl of BCP (Sigma) per 1 ml of TRIZOL reagent were added. Samples were vigorously vortexed for 15 seconds and incubated at room temperature for 2 to 3 minutes. Samples were centrifuged at 13000 rpm for 15 minutes at 4°C. Following centrifugation, the mixture separates into lower red, phenol-chloroform phase, an interphase, and a colourless upper aqueous phase. RNA remains exclusively in the aqueous phase. The upper aqueous phase was transferred carefully into a fresh tube without disturbing the interphase.

The RNA was precipitated by mixing the aqueous phase with 500 µl of isopropanol (Sigma). The mixture was incubated for 10 minutes at room temperature and centrifuged at 13000 rpm for 30 minutes at 4°C. The supernatant was removed completely and the RNA pellet was washed once with 75% ethanol, adding at least 1 ml of 75% ethanol per 1 ml of TRIZOL Reagent used for the initial homogenization. The samples were mixed by vortexing and centrifuged at 8000 rpm for 5 minutes at 4°C. The washing procedure was repeated twice and afterwards, ethanol was completely removed. The pellet was then air-dried and dissolved in RNase free water.

2.3.2 TURBO Dnase Treatment

For the detection of *LINC1* by real-time quantitative PCR (RT-qPCR) the RNA samples were treated with DNase (TURBO DNA-free TM Kit, ambion by life

technologies) to remove contaminating genomic DNA. The reaction volume was 20µl with an RNA concentration of 200 ng/µl,. 2 µl of TURBO DNase Buffer and 1 µl TURBO DNase were added to the RNA and mixed gently. After incubation at 37 °C for 30 min, 2 µl of DNase Inactivation Reagent was added followed by incubation for 5 min at room temperature. During the incubation period tubes were flicked 2-3 times to redisperse the DNase Inactivation Reagent. Samples were centrifuged at 10,000 x g for 5 min and RNA was transferred to a fresh tube. RNA quantity was determined by measuring the absorbance at 260 nm using a BioPhotometer or Nanodrop. Purity was assessed by the ratio of A260 nm/A280 nm and A260 nm/A230 nm. Only samples with A260 nm/A280 nm ratios between 1.9 and 2.2 and A260 nm/A230nm ratios between 1.6 and 2.5 were used for further experiments. Aliquots of RNA were stored at -80 °C until use. All working steps were performed on ice to minimize the risk of RNA degradation.

2.3.3 Reverse Transcription cDNA synthesis

For mRNA quantification, 1000 ng of total cellular RNA were reverse transcribed using the QuantiTect Reverse Transcription Kit (Qiagen, Hilden, Germany) according to the manufacturer's instructions. First, a genomic DNA elimination step was performed at 42°C. The pipetting scheme for this step is listed in Table 1. The reactions were performed in a Biorad Thermo Cycler (Biorad, Hamburg, Germany). Afterwards the reverse transcription was done using the reaction mix listed in Table 2. The thermal cycling conditions are listed in Table 3.

Table 1: Genomic DNA elimination

Reagents	Volume (µl)
gDNA wipeout buffer (7x)	2
RNase free water (up to 12 µl)	X
RNA (1000ng)	Y
TOTAL	14

Table 2: Mastermix for cDNA synthesis

Reagents	Volume (μl)
QuantiScript Reverse Transcriptase	1
QuantiScript RT Buffer (5x)	4
RT Primer Mix	1
Template RNA (1000ng)	14
TOTAL	20

Table 3: cDNA synthesis: cycling program

Temperatur ($^{\circ}$C)	Time(min)
42	5
95	3

2.3.4 Quantitative real time PCR (qRT-PCR)

Relative mRNA expression levels were measured using the Quantitect SYBR Green PCR kit(Qiagen) according to the manufactures instructions on a Light Cycler480 (Roche Diagnostics, Mannheim, Germany). qRT-PCR was done in duplicates for each sample with specific primers (see Table 6) (Primers were purchased from Eurofins Genomics). For relative gene quantification U6, B2M and TBP were used as housekeeping genes. 2 μ l of diluted cDNA (20 ng) and 23 μ l of mastermix (see Table 4) were added to each well of a 96 well plate (Roche Diagnostics). The thermal cycling conditions are shown in Table 5.

Table 4: Mastermix for qRT-PCR

Reagents	Volume (µl)
Quantitect SYBR Green Master Mix (2x)	12,5
Forward primer (0,4 µM)	1
Reversed primer (0,4 µM)	1
RNasefree water	8,5
Template (10 ng)	2
Total	25

Table 5: qRT-PCR program

Program Name	Cycles	Analysis mode
Pre-incubation	1	None
Amplification	40	Quantification
High Resolution Melting	1	Melting Curves
Cooling	1	None

Target (°C)	Acqu. Mode	Hold (hh:mm:ss)	Ramp rate (°C/s)	Acquisitions (per°C)	Sec. Target (°C)	Step Size (°C)	Step Delay (cycles)
Pre-incubation							
95	None	00:15:00	4,4		0	0	0
Amplification							
94	None	00:00:15	2,2		0	0	0
55	None	00:00:30	2,2		0	0	0
72	Single	00:00:30	4,4		0	0	0
High Resolution Melting							
95	None	00:00:05	4,4				
65	None	00:01:00	2,2				
97	Continuous			10			
Cooling							
40	None	00:00:10	2,2		0	0	0

Table 6: Primer sequences for qRT-PCR

LINC1_fw AAGGGGCAAAGGAAGCTGTAA
LINC1_rev TCTCCCGTAAGTGCTGTGAG
U6_fw CTCGCTTCGGCAGCACACA
U6_rev AACGCTTCACGAATTTGCGT
B2M_fw TCTCTGCTCCCCACCTCTAAGT
B2M_rev TCTCTGCTCCCCACCTCTAAGT
TBP_fw TGCACAGGAGCCAAGAGTGAA
TBP_rev CACATCACAGCTCCCCACCA

2.3.5 Calculation of relative gene expression

Changes in mRNA or miRNA expression levels of the gene of interest in treated samples relative to their controls were determined using the $\Delta\Delta\text{Ct}$ -method. ΔCt was calculated by subtracting the Ct-value of the housekeeping gene from the Ct-value of the gene of interest. ΔCt -value of control samples were subtracted from the ΔCt -value of the analysed samples to obtain the $\Delta\Delta\text{Ct}$ -value. $2^{-\Delta\Delta\text{Ct}}$ was calculated to illustrate the results in a graph (78).

$$\Delta\text{Ct} = \text{Ct gene of interest} - \text{Ct housekeeping gene}$$

$$\Delta\Delta\text{Ct} = \Delta\text{Ct sample} - \Delta\text{Ct control}$$

2.4 Western Blot analysis

2.4.1 Protein Isolation

Total proteins from stably or transiently transfected CRC cells were extracted with radioimmunoprecipitation assay (RIPA) buffer (150 mM NaCl, 50 mM Tris-HCl, pH 7.5, 1% Triton, 0.1% SDS, 0.1% sodium deoxycholate and 1% Nonidet P40). First, cells were washed with PBS and trypsinized. Detached cells were resuspended in

culture medium, collected in a 15ml falcon and centrifuged for 5 min at 800 rpm. The cells were again washed twice with cold PBS and 100-300 μ l of RIPA buffer supplemented with 0,1 M DTT (Sigma) 1 M PMSF (Sigma) and Protease inhibitor cocktail (Thermo Scientific, Rockford, IL) were added to the cell pellet. Cells were incubated with RIPA buffer for 30 minutes and vortexed every five minutes for complete cell lysis. Afterwards, the cell lysate was centrifuged for 15 minutes at 13.000 rpm and the supernatant containing the cellular proteins was transferred to a fresh Eppendorf tube. Total protein concentration was measured using the Pierce 660 nm protein assay (Thermo Scientific) according to the manufacturer recommendations.

2.4.2 SDS PAGE and wet transfer

20 μ g of total cellular proteins were supplemented with 2x sample loading buffer and heated for 10 minutes at 65°C. Afterwards, protein extracts were subjected to electrophoresis on a 4–15% Mini-PROTEAN® TGX™ Precast Gel (Biorad, Hercules, CA). In addition 10 μ l of Precision Plus Protein Prestained Standards (Bio-Rad) were loaded onto the gel to identify protein molecular weights. Proteins were separated at 150 V for one hour using 1x running buffer (25mM Tris, 192mM glycine, 0.1% SDS, Biorad). Afterwards proteins were transferred onto a nitrocellulose membrane (Biorad) at 90 V for 1.5 hours using 1x transfer buffer (25mM Tris, 192mM glycine, 20% ethanol, Biorad). To evaluate the quality of the transfer, the membrane was stained with ponceauS (Sigma).

2.4.3 Detection of protein expression

The membrane was blocked for 1 hour with 3% non-fat dry milk in Tris buffered Saline/0.1% Tween-20. Immunoblotting was performed and the apoptosis marker PARP (Cell Signaling, Cat.No. 9542) and β -Actin (Sigma, Cat.No. A5441, clone AC-15) were detected using HRP-conjugated anti-mouse or anti-rabbit antibodies,

respectively (Dako, Glostrup, Denmark). Visualization was performed using an enhanced chemoluminescence detection system (Super Signal West Pico, Thermo Scientific, Rockford, IL).

2.4.4 Detection of β -actin protein expression

To normalize protein expression levels, β -actin expression was detected on the membrane. Therefore, the membrane was stripped using Restore Western Blot Stripping Buffer (Thermo Scientific, Rockford, IL) and reprobbed with a monoclonal anti- β -actin antibody (Sigma, diluted 1:5000 in 1% (v/v) blocking solution) overnight at 4°C. The membrane was washed three times with TBS-T (Biorad) for 15 min followed by incubation with HRP-conjugated rabbit-anti-mouse antibody (Dako, Glostrup, Denmark) for two hours at room temperature. Three washing steps for 15 min with TBS-T (Biorad) and immunodetection as described above were performed (see section 3.4.3).

2.4.5 Relative quantification of protein expression

Relative quantification of protein expression was performed using the ImageJ (NIH, Bethesda, Maryland) software. Therefore, the band density of the protein of interest was measured and divided by the density of the loading control beta actin.

2.4.6 Xenograft mouse model

For tumor xenograft experiments, 7 female, five week-old NOD/SCID mice were obtained from Charles River Breeding Laboratories (Sulzfeld, Germany). They were transiently transfected. *LINC1* siRNA₁ or scrambled control HCT116 cells were resuspended in 100 μ l of phosphate-buffered saline (PBS) and then mixed with 100 μ l of Matrigel (BD, Franklin Lakes, NJ) and subcutaneously injected at a density of 6×10^5 cells into the flanks of mice. Animals were sacrificed 21 days after injection. Tissues were fixed in 4% buffered formaldehyde for 24 hours, paraffin-embedded and stained by hematoxylin-eosin (HE). All animal work was done in accordance with

a protocol approved by the Institutional Animal Care and Use Committee at the Austrian Federal Ministry for Science and Research.

2.5 Statistical analysis

All statistical analyses were performed using SPSS version 20 software (SPSS Inc., Chicago, IL, USA) or MedCalc software (version 13.1.2.0). Student t-test or non-parametric tests were used where appropriate. For all calculations, $p < 0.05$ was considered as significant.

3 Results

3.1 LINC1 Expression analysis in CRC cell lines

A qRT-PCR was performed to examine the LINC1 expression patterns in different human CRC cell lines. The expression levels were analysed in HCT116, HRT-18, SW480, DLD1, Caco-2, RKO, SW48 and HT29 (Figure 1). Based on these results we selected HCT116, HRT-18, SW480 and DLD1 cells for further investigations.

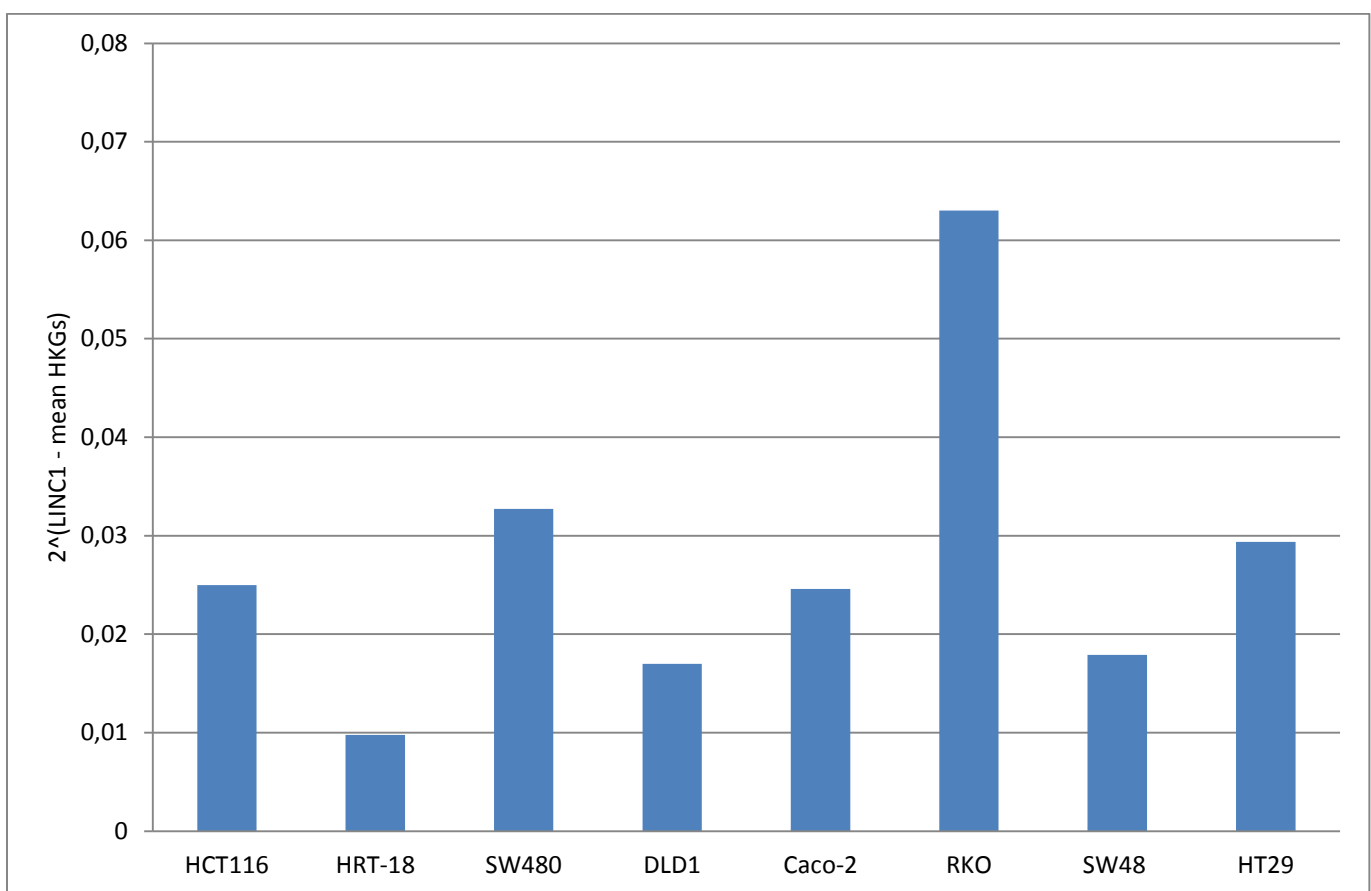


Figure 1: Relative expression levels in CRC cell lines. Bar charts graph shows the expression levels of LINC1 in eight different CRC cell lines as measured by qRT-PCR. The expression was detected in all tested 8 cell lines. The housekeeping genes B2M and TBP were used for normalization. The relative gene expression levels were calculated using a standard $2^{-\Delta\Delta CT}$ method. Values are presented as the mean \pm standard deviation (SD) of technical duplicates.

3.2 Establishing knock down technique for LINC1

To study the biological effects of expression changes and reduce the endogenous expression levels of *LINC1*, CRC cell lines HCT116, HRT-18, SW480 and DLD1 were transiently transfected with two different siRNAs or a control-non silencing siRNA, respectively. The successful siRNA mediated knock down of *LINC1* was then verified by qRT-PCR (Figure 2). Compared to the negative control *LINC1* expression was significantly decreased in HCT116 (Fig. 2-A), HRT-18 (Fig.2-B), SW480 (Fig.2-C) and DLD1 (Fig.2-D). (* = significant, $p < 0.05$; **, $p < 0.01$; ***, $p < 0.001$).

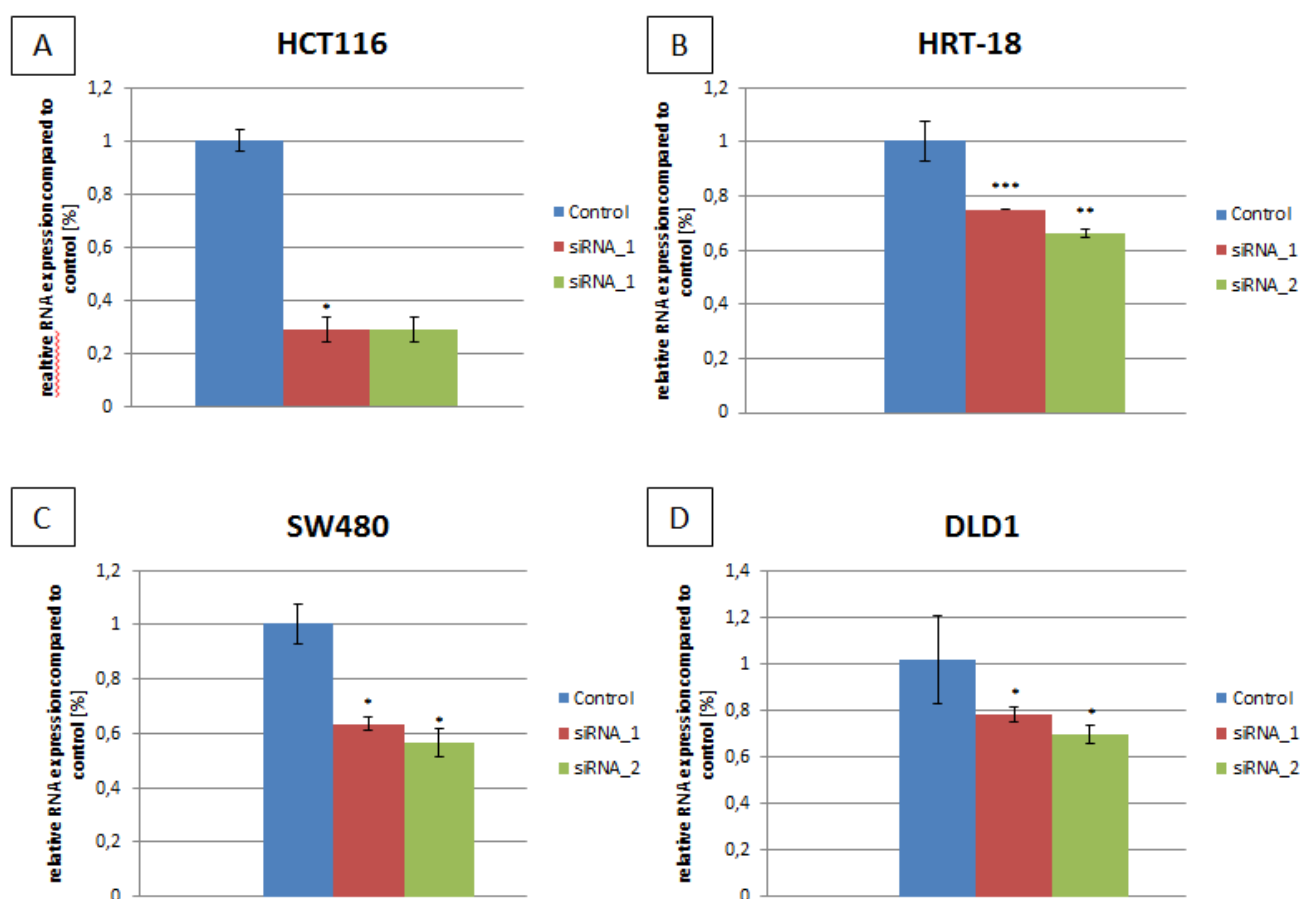


Figure 2: Knock down of *LINC1* in CRC cell lines. Expression levels of *LINC1* in HCT116 (A), HRT-18 (B), SW480 (C) and DLD1 (D) 48 hours after

transfection with 50 n M siRNA_1, siRNA_2 and control siRNA were analysed by RT-qPCR. Reactions were performed in technical duplicates. The housekeeping gene U6, B2M and TBP were used for normalization and relative gene expression levels were calculated using a standard $2^{-\Delta\Delta CT}$ method. The data represent the results of three technical replicates. (p-value <0.05 considered as significant).

3.3 Colony forming unit assay

To evaluate the growth potential of *LINC1* silencing in the CRC cell lines, colony forming units assay was performed. The data shows that *LINC1* knock down inhibits the ability to form single colonies in the cell lines HCT116, HRT-18, SW480 and DLD1. Compared to control cells, transient transfection of *LINC1* siRNA resulted in a significant reduction of the colony number (Fig.3).

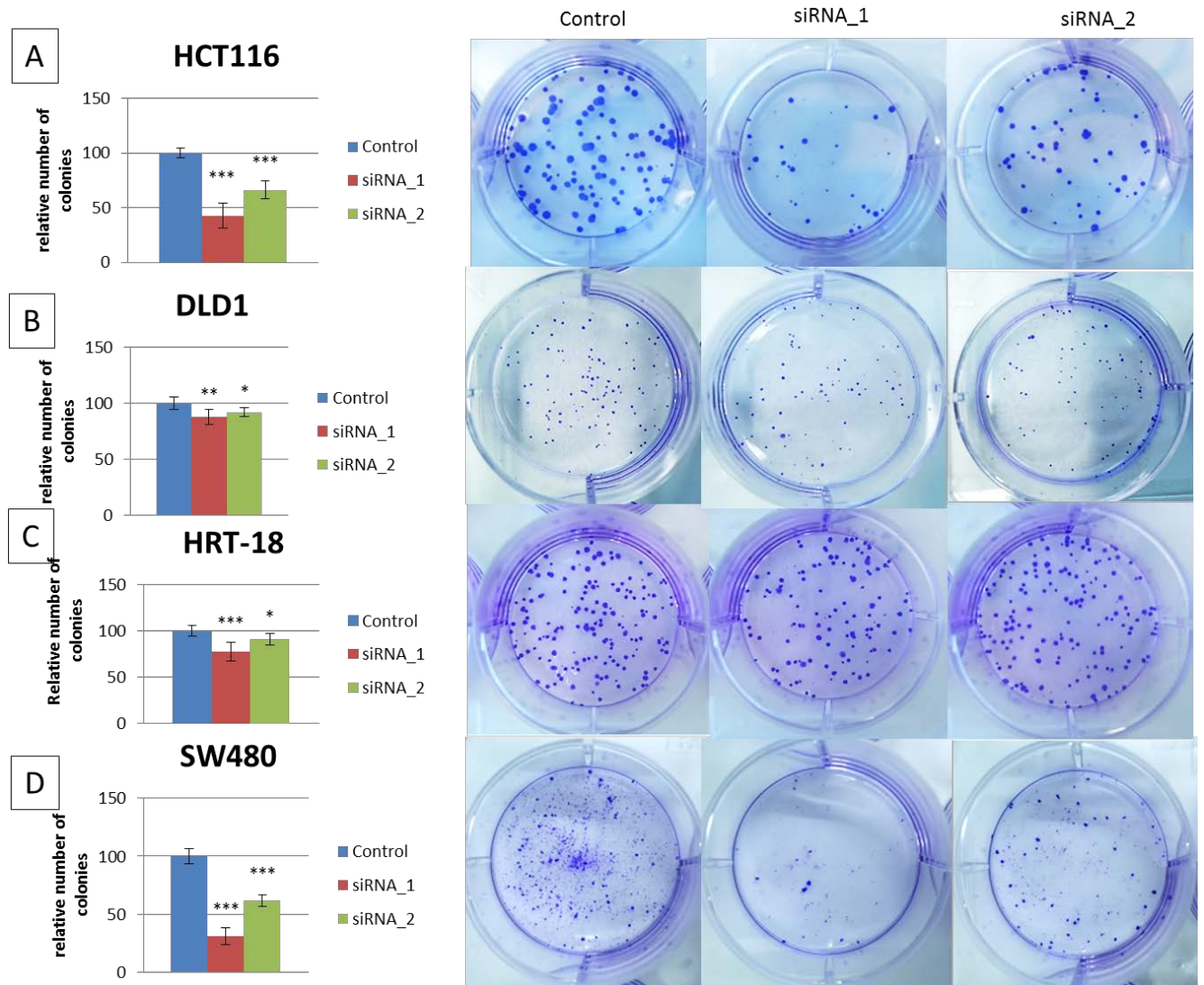


Figure 3: Colony forming unit assay. The relative number of colonies compared to the control showed a significant reduction in colony formation of *LINC1* silencing in the HCT116 (A), DLD1 (B), HRT-18 (C) and SW480 (D) cell lines. Transfected cells were cultured in 6 well plates and then stained with crystal violet solution. (p-value <0.05 considered as significant).

3.4 Soft Agar Assay

The soft agar assay is commonly used to determine anchorage-independent growth. In the soft agar assay, a significantly lower number of colonies in *LINC1*-silenced cells compared to control cells for all four CRC cell lines was observed (Fig.4).

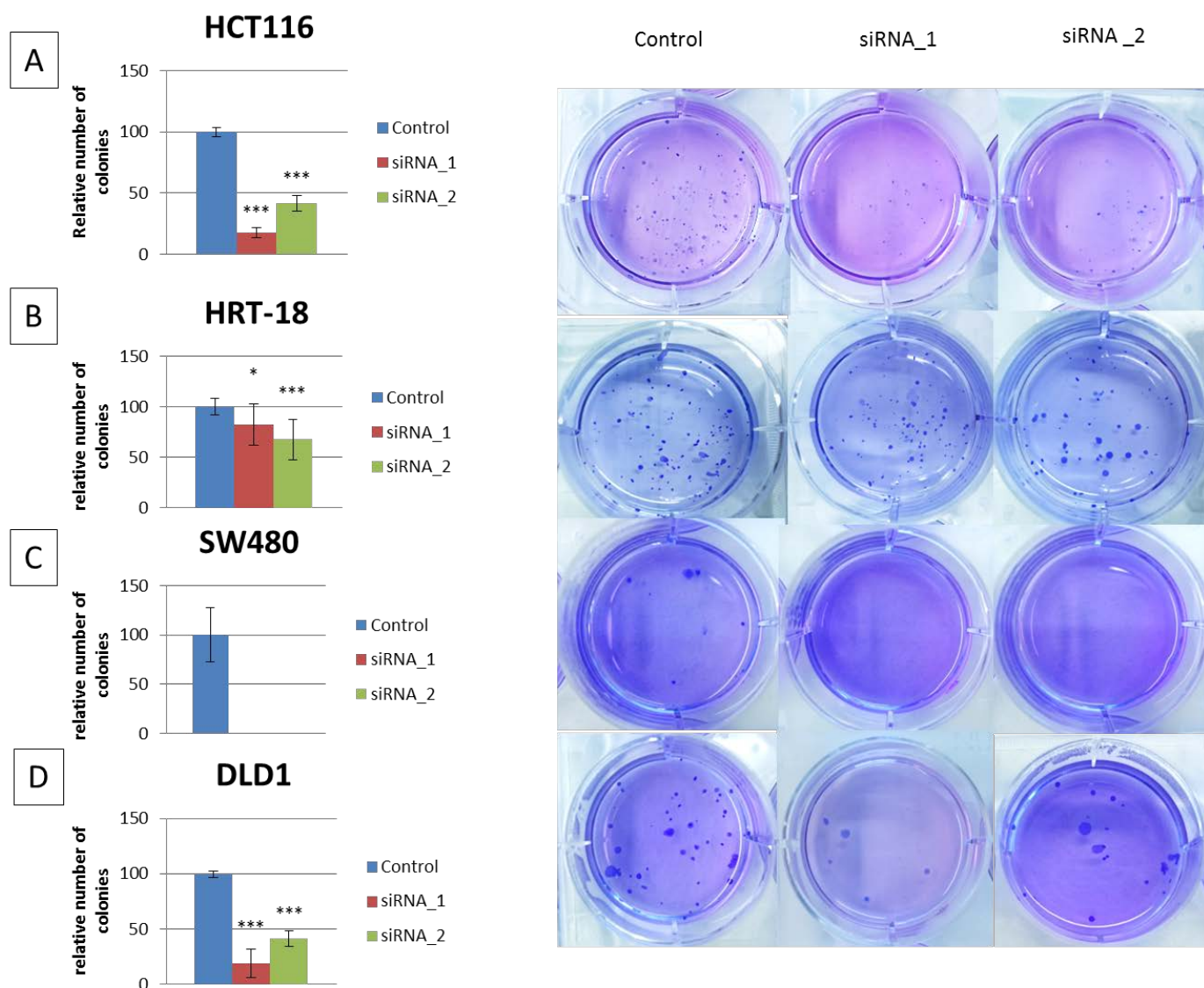


Figure 4: Soft Agar Assay. *LINC1* downregulation suppresses anchorage-independent growth in soft agar. The transient transfected cells were cultured in 6 well plates in 6 technical replicates and then stained with crystal violet solution. A significant lower capability of colony formation under soft agar conditions in the CRC cell lines HCT116 (A), HRT-18 (B), SW480 (C) and DLD1 (D) was found in *LINC1* silenced cells compared to control cells. (p-value <0.05 considered as significant).

3.5 WST-1 Proliferation Assay

After confirming a successful transient silencing of *LINC1* we checked whether *LINC1* levels have an impact on cellular growth by performing a WST-1 cellular proliferation assay. We measured the proliferation rates after 24h, 48h, 72h and 96h in four different CRC cell lines transiently transfected with siRNA_1, siRNA_2 or non-silencing siRNA. In the cell lines HCT116, HRT-18, SW480 and DLD1 a significant reduction in cellular growth after 96h was detected (Fig.5 A-D).

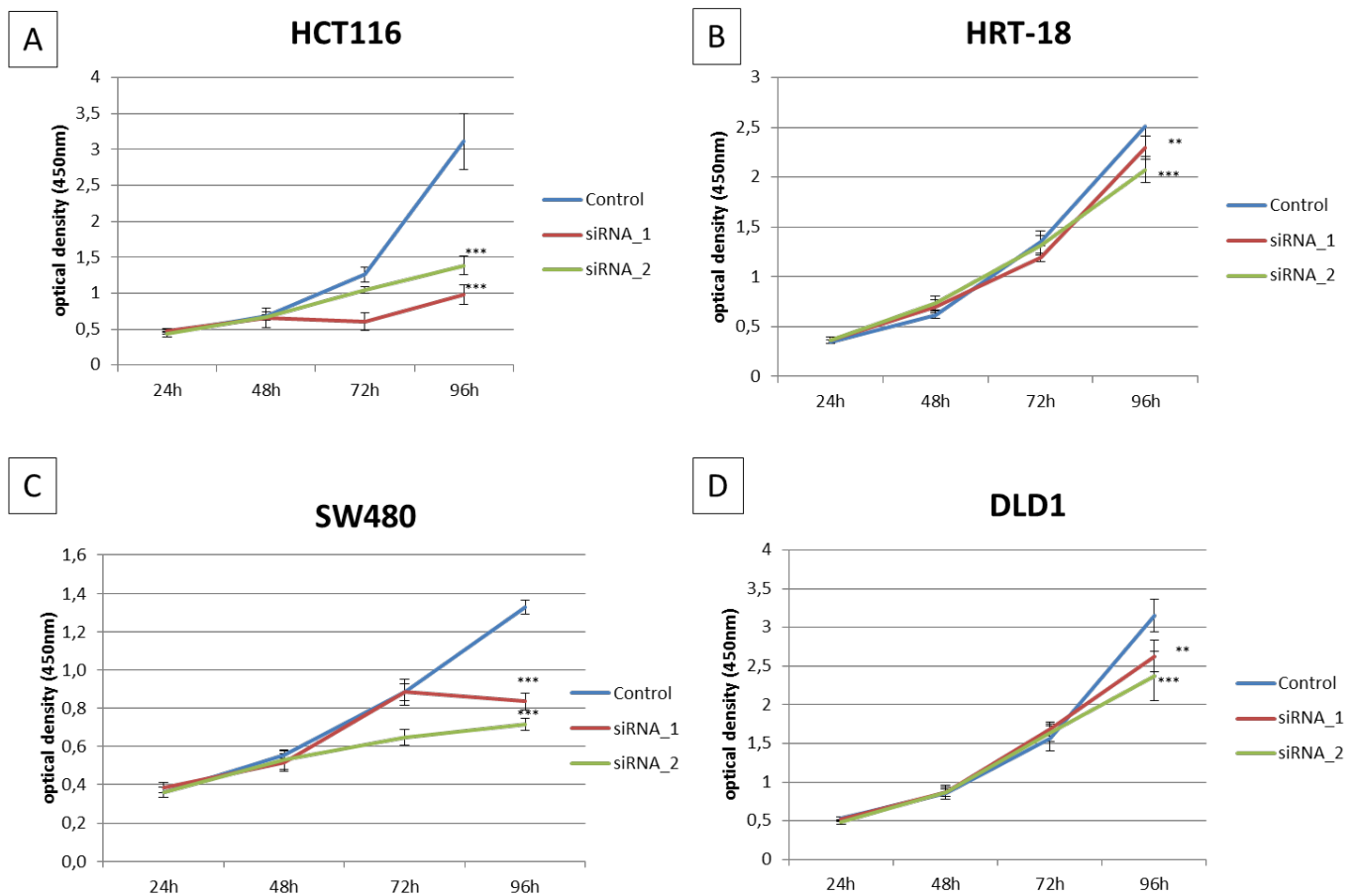


Figure 5: WST-1 Proliferation assay. *LINC1* silencing decreases cellular growth rates. The effect of *LINC1* silencing in CRC cell lines on cellular growth was observed using WST-1 proliferation assays. In the cell lines HCT116 (A), HRT-18(B), SW480 (C) and DLD1 (D) a significant decrease of cellular growth after 96 hours is shown. (p-value <0.05 considered as significant).

3.6 Tumorsphere formation assay

Furthermore, we investigated the effect of *LINC1* mediated knock down on the self-renewal capacity by using a tumorsphere formation assay under ultra-low attachment conditions. In the CRC cell lines HCT116, SW480 and DLD1 the number of tumorspheres was significantly lower ($p < 0.05$) in *LINC1*-silenced cells (Fig.6 A-C). In HRT-18 cells we could not detect any formation of tumor spheres neither in the control nor in the *LINC1* silenced cells.

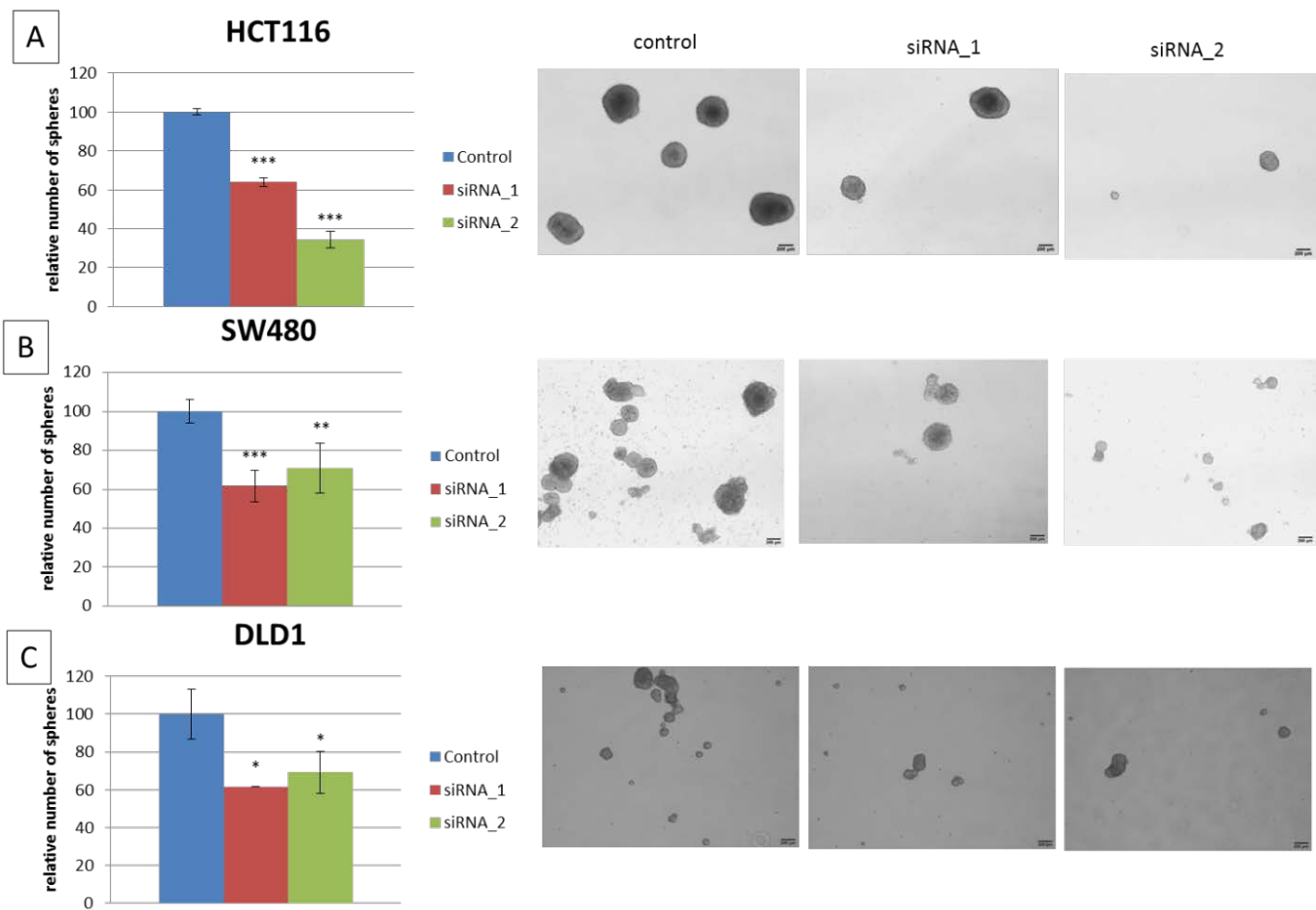


Figure 6: Tumorsphere formation assay. Graphs represent the results from 6 technical replicates of the CRC cell lines HCT116 (A), SW480 (B) and DLD1 (C) of transiently transfected cells with siRNA_1 or siRNA_2 against *LINC1* compared to control cells. In each cell line, a significantly decreased number of colonies was observed in the *LINC1*-silenced cells. (p -value < 0.05 considered as significant).

3.7 Wound healing scratch assay

To monitor cell migration a wound healing assay was performed. Transient transfection of the CRC cell lines HCT116, HRT-18, SW480 and the measurement of the scratch closure after 24 hours and 48 hours showed that the control cells closed the scratch significantly earlier than the *LINC1* knock down cells (Fig. 7 A-C).

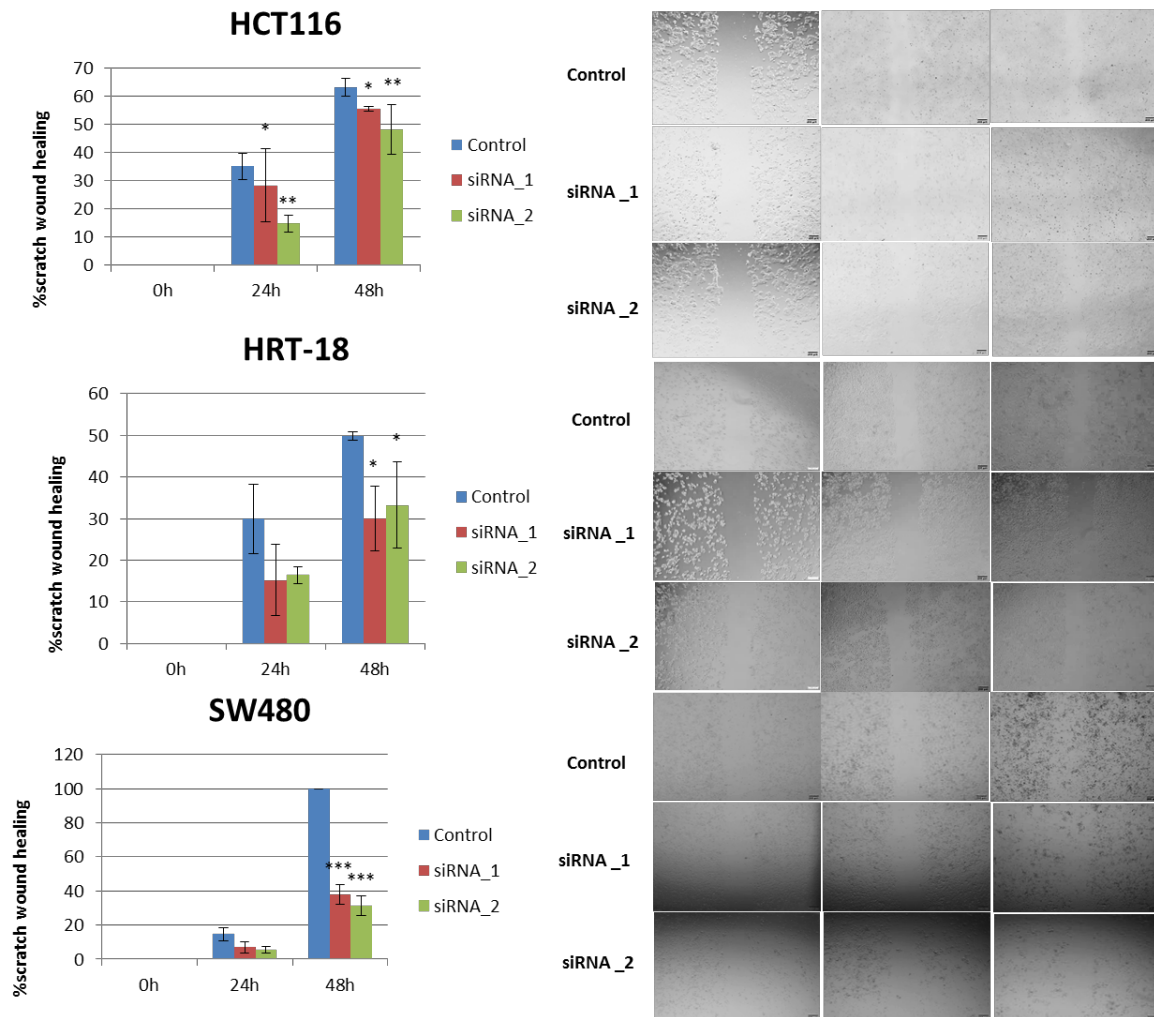


Figure 7: Wound healing scratch assay. Pictures demonstrating scratch wound healing assay in HCT116 (A), HRT-18 (B) and SW480 (C) cells after transient transfection of *LINC1* with siRNA_1, siRNA_2 or respective control. 0h=scratch at the beginning; 24h=scratch after 24 hours; 48h= scratch after 48 hours. Bar charts graphs showing the results of measurement of scratch closure after 24 hours and 48 hours for the *LINC1* silencing CRC cells. The control cells closed the scratch significantly earlier than the *LINC1* silenced cells. (p-value <0.05 considered as significant).

3.8 Apoptosis Assay Caspase 3/7

Since *LINC1* silencing led to a decrease of cancer cell growth, we were interested whether this phenotype can be explained by induction of apoptosis by caspase enzymes. Hence we performed a caspase 3/7 apoptosis assay after transient knock down of *LINC1* in the HCT116, SW480 and DLD1 cells. After 48 hours and 96 hours we observed a significantly increased Caspase 3/7 activity in *LINC1* silenced cells compared to control cells (Fig. 8 A-C).

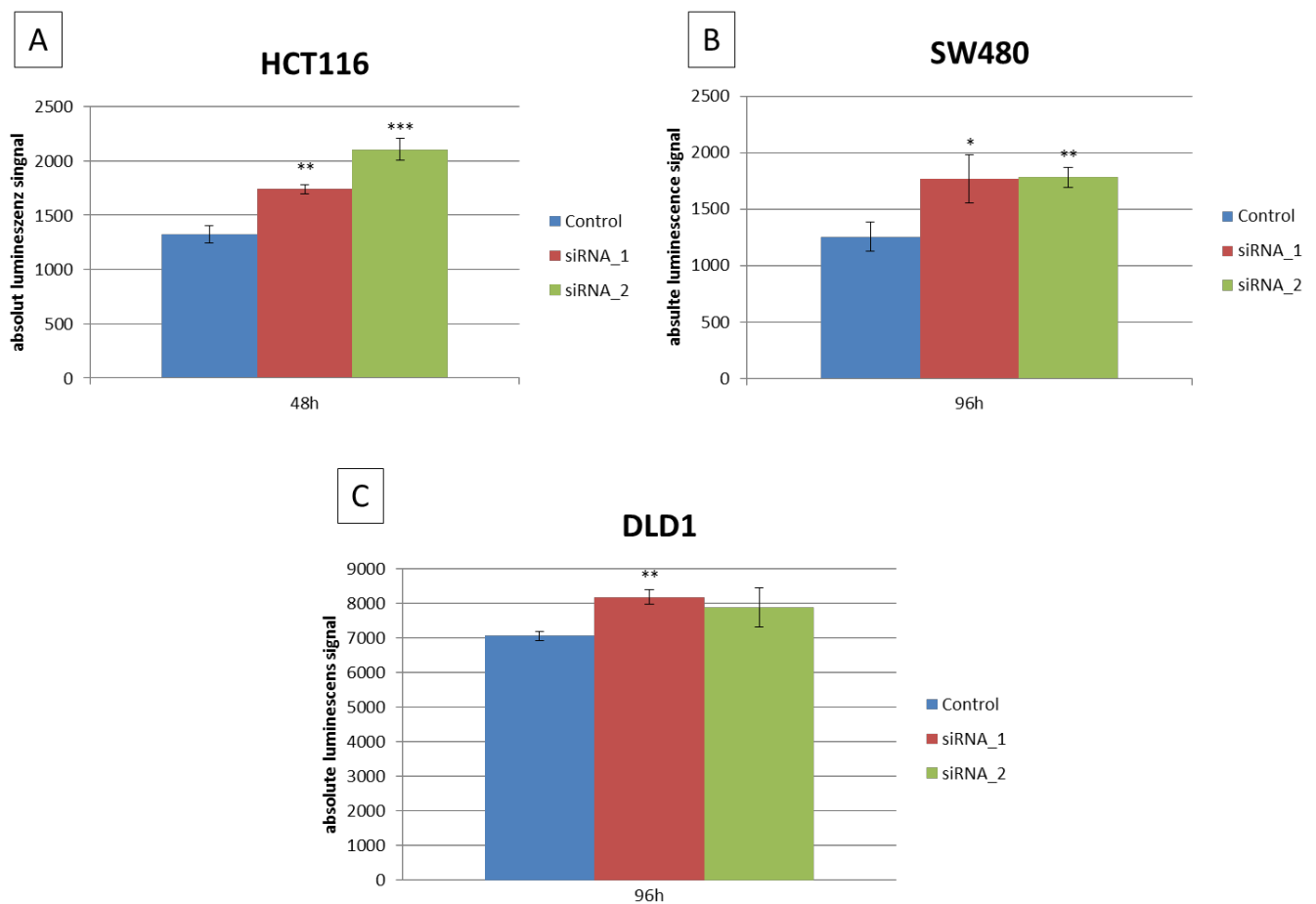


Figure 8: Apoptosis assay. To examine the apoptosis rates in the cell lines HCT116 (A), SW480 (B) and DLD1 (C) Caspase 3/7 assay were performed. Cells were cultured in 96 well plates with siRNA_1, siRNA_2 and non-silencing siRNA. After 48 hours and 96 hours the caspase reagent was added and luminescence was measured. The data was generated by three technical replicates. (p-value <0.05 considered as significant).

3.9 Western Blot PARP

In addition, this pro-apoptotic phenotype was further examined by measuring the cleaved PARP protein expression by Western Blot analysis 48h and 72h after transient knock down of *LINC1*. We detected the cleaved PARP molecule 48h and 72h after transient transfection with *LINC1* siRNAs in all tested cell lines confirming that low *LINC1* levels lead to increased apoptotic activity in CRC cell lines (Fig.9 A-C).

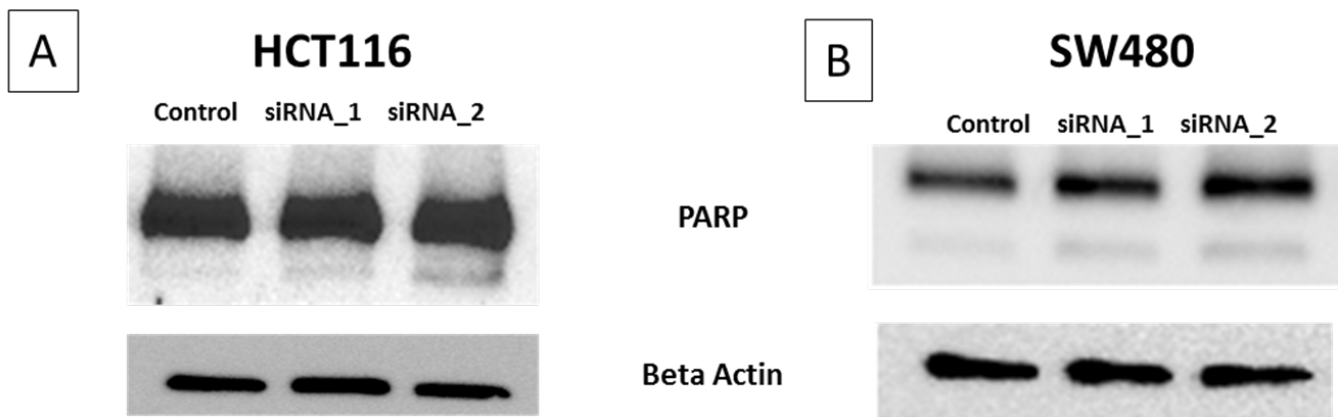


Figure 9: Western Blot PARP detection in *LINC1* silenced CRC cell lines. The cleaved PARP molecule could be detected in the cell lines HCT116 (A) and SW480 (B). Beta-actin was used as loading control.

3.10 Cell cycle analysis

Subsequently, we performed a cell cycle analysis assay, using propidium iodide staining and FACS analysis, to clarify if *LINC1* knock down suppresses colony formation as a result of the inhibition of cell cycle progression. In both cell lines HCT116 and SW480 the *LINC1* silencing slightly increased the population in the G1-phase of the cell cycle (Fig.10 A-B).

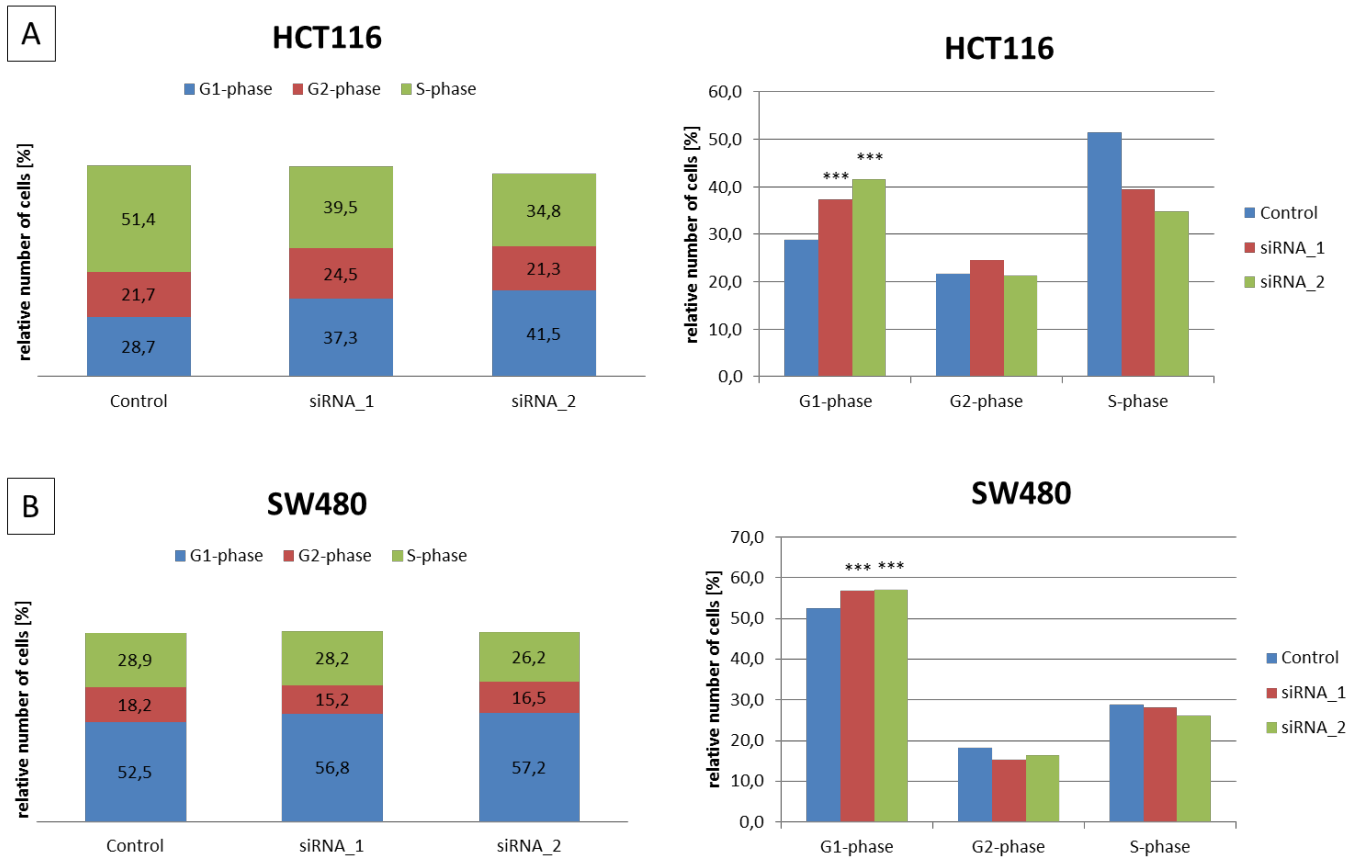


Figure 10: Cell cycle analysis. *LINC1* silencing results in a significant alteration of cell cycle distribution in HCT116 (A) and SW480 (B) cell lines. The phase distributions were plotted relative to the total number of cells. Data was generated by using three biological replicates. (p-value <0.05 considered as significant).

3.11 Xenograft mouse model

To confirm our biological *in vitro* findings *in vivo*, we evaluated the reduced tumor growth in nude mice that were subcutaneously injected with *LINC1* silenced HCT116 cells. The histologically examination of tumor tissue sections revealed no significant difference between the control group and the *LINC1* silenced groups (Fig.11).

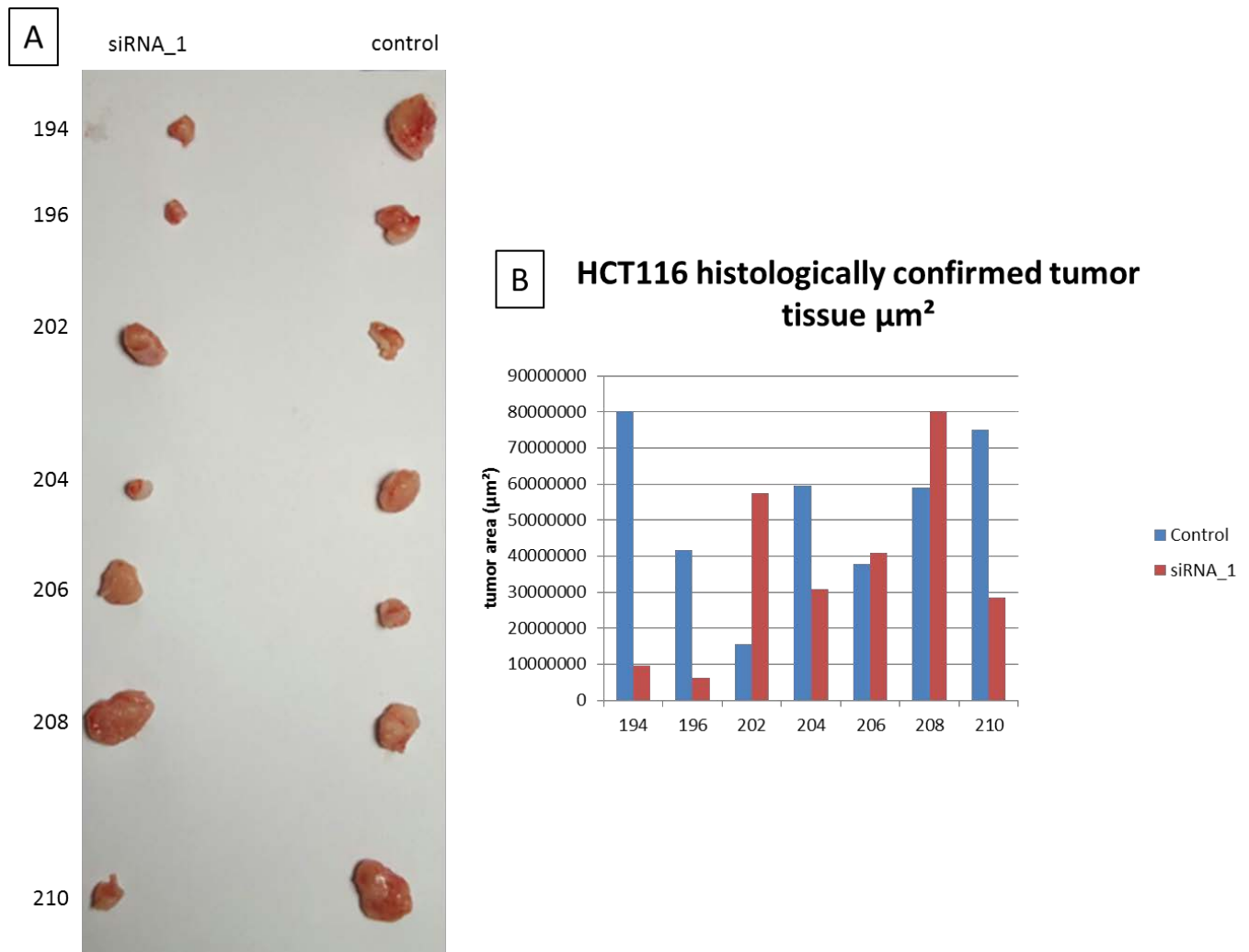


Figure 11: Xenograft mouse model. Histologically confirmed tumor tissue. HCT116 cells were subcutaneously injected, at a density of 6×10^5 cells into seven female NOD/SCID mice. Either transiently transfected *LINC1* siRNA_1 or scrambled control cells were injected into the flanks of mice. No significant contrast in tumor growth was shown between the control cells and the *LINC1* silenced cells (A,B).

However, we could confirm differences in the maximal diameter tumor tissue showing more vital tumor tissue in the control group than in the *LINC1* downregulated group (Fig. 12).

HCT116 maximal diameter tumor tissue

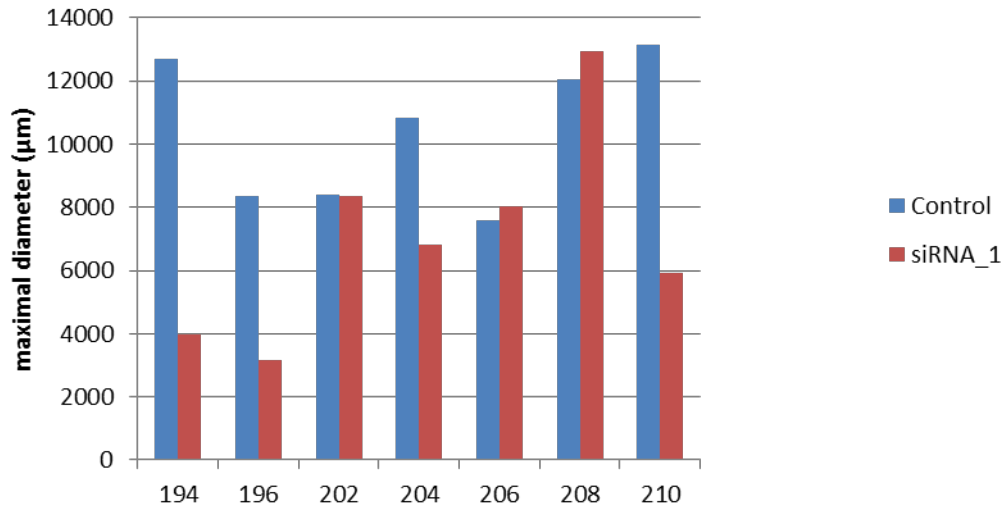
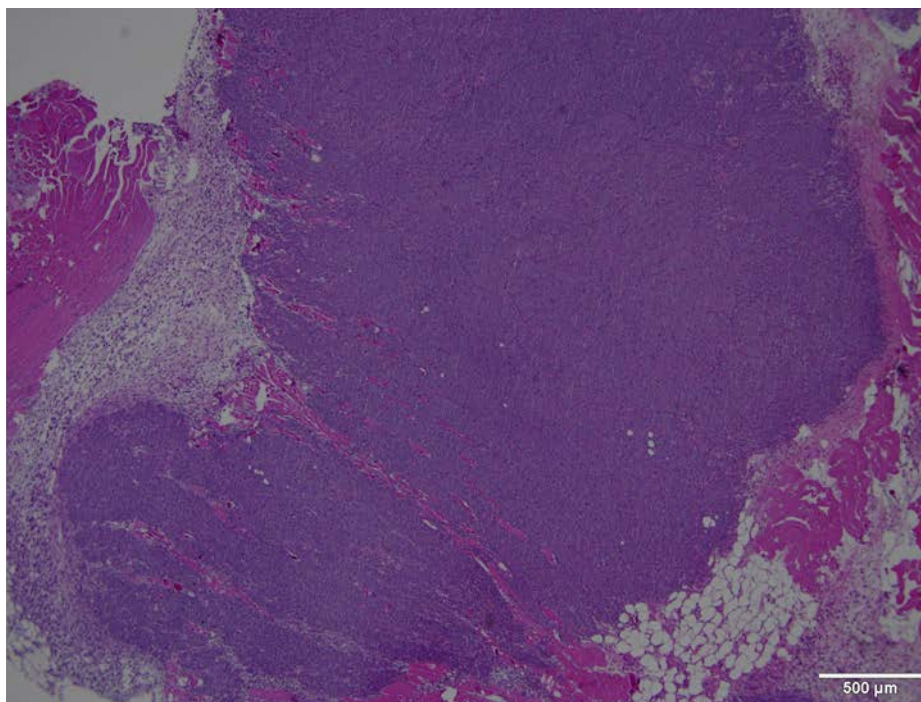


Figure 12: Xenograft mouse model maximal diameter tumor tissue. Measurements of the maximal diameter from formalin fixed tumor tissues stained with HE shows a slight difference in the tumor size in the control group compacted to LINC1 silencing group.

196_Control



196_siRNA_1

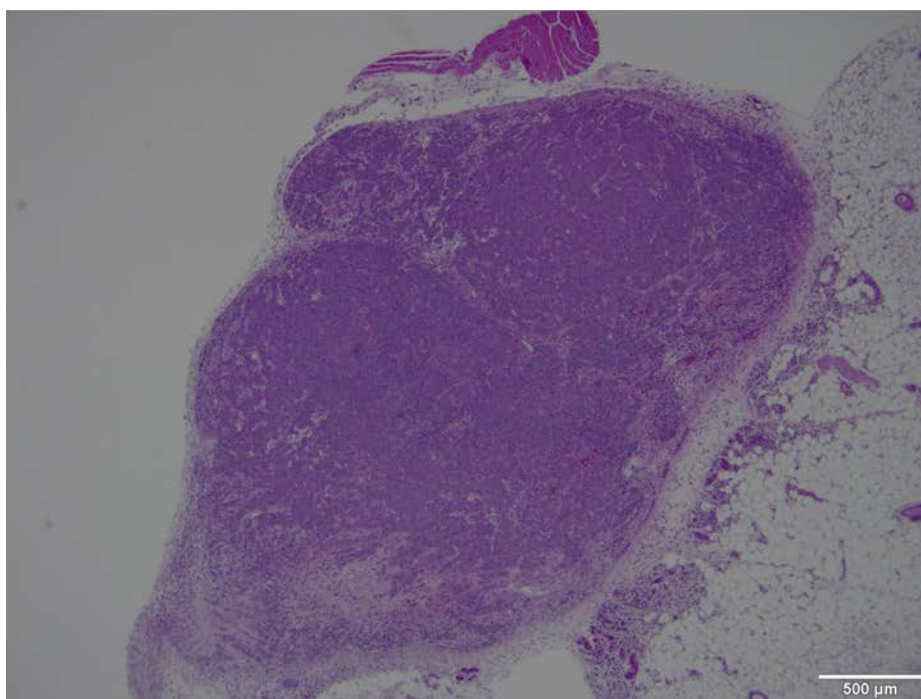


Figure 13: Representative picture of HE stained FFPE xenograft tumor tissues. Picture showing a representative picture of one xenograft mouse injected with scrambled control cells (upper picture) or silenced *LINC1* cells (lower picture). The tissues were fixed in 4% buffered formaldehyde for 24 hours, afterwards paraffin-embedded and then stained by HE.

4 Discussion

Colorectal cancer is one of the most common causes of cancer related death worldwide (1). Chemotherapeutic drugs such as 5-fluorouracil remain the main established treatment for patients who suffer from CRC (16-18). Therefore it is of strong clinical interest to find novel prognostic biomarkers which might predict the prognosis and progression in colorectal cancer patients.

LncRNAs are commonly defined as endogenous cellular RNAs molecules longer than 200nt in length with limited or no protein-coding capacity and capable of regulating gene expression (79) at different levels, including transcription, chromatin modification and post-transcriptional processing (80-82). Due to their role as key regulators of gene expression lncRNAs have moved into the spotlight of research (35, 83).

The aim of this master's thesis was to investigate the biological function of the novel lncRNA *LINC1* and its impact on the malignant behaviour of CRC *in vitro* and *in vivo*. Therefore we examined the effect of *LINC1* on several hallmarks of cancer.

First, we selected four CRC cell lines (HCT116, HRT-18, SW480 and DLD1) to examine the effects of *LINC1* silencing on biological behaviour and cell phenotype. This four cell lines were chosen because of their high *LINC1* expression levels. For siRNA silencing two independent siRNAs were used to investigate a consistent phenotype and to exclude possible off target effects. This effects can also concern the monitored phenotype, like cellular growth which is regulated by many other genes (84). SiRNAs are 21 – 25 bp long double stranded RNA molecules that operate through a process termed RNAi, can bind to complementary nucleotide sequences, leading to degradation of mRNA and hence downregulation of their targets (85). To ensure targeted knock down we worked with two different siRNAs, namely siRNA_1 and siRNA_2 that bind to different regions of *LINC1*. The efficient knock down was confirmed in all four cell lines by RT-qPCR. The various silencing capabilities in the cell lines may be provoked by the different binding position of the siRNAs on the target RNA or by inherent biological or technical variability of such experiments (86). Subsequently, the role of *LINC1* in CRC cell lines was examined by analysing the alterations of biological behaviours after silencing.

To evaluate the influence on cellular growth after *LINC1* silencing colony formation assay was performed (87). In all four CRC cell lines we could show significantly lower numbers of colonies compared to the control, due to *LINC1* silencing.

Furthermore, to confirm this result with a second independent method, we performed a WST-1 proliferation assay. The assay showed that *LINC1* silencing has an impact on cellular growth in all four cell lines and also revealed a significant decrease in the proliferation rate due to *LINC1* silencing.

Another hallmark of cancer is the competence of anchorage-independent growth. It is a well-established method for characterizing this ability *in vitro* and is considered to be one of the most stringent tests for malignant transformation in cells (88). It also allows semi-quantitative evaluation of this capability in response to *LINC1* silencing. Under this semisolid agar conditions the CRC cell lines HCT116, HRT-18, SW480 and DLD1 revealed in a significantly lower capability of colony formation after *LINC1* silencing compared to the control.

To sum up the knock down of *LINC1* resulted in a decrease of colony formation, proliferation and the ability of anchorage-independent growth. This indicates a role in the modulation of cellular growth.

To further investigate if reduced proliferation and colony formation, as a result of *LINC1* silencing is mediated through induction of apoptosis, we performed a caspase 3/7 apoptosis assay. In the CRC cell lines HCT116, SW480 and DLD1 a significant difference in Caspase 3/7 activity in *LINC1* silenced cells was detected compared to control cells. This result indicates that this effect might be caused by the induction of apoptosis. In addition we examined the pro-apoptotic phenotype by measuring the cleaved PARP protein expression by western blot analysis 48h and 72h after transient downregulation of *LINC1*. The cleaved PARP molecule was detected after 48h and 72h after transient transfection with *LINC1* siRNAs in the cell lines HCT116, SW480 and DLD1 confirming that low *LINC1* levels lead to increased apoptotic activity in CRC cell lines. A previous study showed that the downregulation of long non coding RNA BLACAT1 inhibits proliferation and induces cell apoptosis *in vitro* in the CRC cell lines HCT116 and SW480(89).

Moreover, we examined if impaired cellular growth and colony formation may be caused by inhibition of cell cycle progression. Therefore we performed a propidium

iodide staining and FACS analysis, to clarify if *LINC1* knock down suppresses colony formation as a result of the inhibition of cell cycle progression. Deregulation of the cell cycle is a hallmark of cancer. The cell cycle consists of three different phases: G0/G1, S and G2/M (90). The CRC cell lines HCT116 and SW480 exhibited significant changes in the cell cycle phase distribution of downregulated cells compared to control cells in all three biological replicates. *LINC1* silencing led to an increase of cells in the G1-phase, indicating that suppressed proliferation and colony formation may be mediated by G1-phase arrest. Key players in the progression and regulation of the cell cycle are cyclins (90, 91). The transition from G1 to S phase is regulated by cyclin depending kinase inhibitors (CDKNs). These inhibitors can bind and thus inactivate the cyclins, resulting in G1 phase arrest (92). It is already shown that gene such as CDKN1A or Cyclin D1 is a critical molecule for regulating cell proliferation in CRC cells (93). However, further analysis must be done to verify our observation such as measurement of mRNA levels of proliferation markers as a good indicator of gene regulation (94, 95).

According to the cancer stem cell hypothesis, tumors are hierarchically organized with a small group of cells which exhibit characteristics related to normal stem cells. These cancer stem cells are culpable for cancer evolution and may set up tumors through the stem cell property of self-renewal. They are considered to cause relapse and metastasis by giving rise to new tumors and are therapy resistant (96). To investigate if *LINC1* expression correlates with cancer stemness a CRC tumorsphere formation assay was performed under ultra-low attachment conditions. In the cell lines HCT116, SW480 and DLD1 we could confirm a significant reduction of tumor spheres after *LINC1* silencing compared to control cells-

Furthermore we monitored whether cancer cell migration and invasion are influenced by *LINC1*. For this purpose we used three independent CRC cell lines. This assay is an elementary and well-developed method to measure cell migration *in vitro* (97). The assay was performed with three biological replicates and we observed a highly consistent phenotype of decreased cancer cell migration in CRC with reduced *LINC1* expression. In order to identify a possible molecular mechanism that might explain this impaired metastatic behaviour further analysis has to be done. A study by YU et al. has already shown that *linc-UFC1* silencing effectively suppressed proliferation *in*

vitro, complementary with induction of cell cycle arrest, apoptosis and metastatic inefficiency (98).

Finally to confirm our *in vitro* findings in an *in vivo* we performed tumor xenograft experiments with nude mice. Therefore, nude mice were subcutaneously injected with transiently transfected *LINC1* silenced HCT116 or control cells. The *in vivo* findings support our *in vitro* data showing that the maximal diameter of vital tumor tissue is significantly decreased in *LINC1* silenced cells compared to control cells. However we could not confirm a significant difference between the tumor growth of *LINC1* silenced cells compared to control cells. This result indicates that the silencing effect of *LINC1* does not have any impact on the cellular growth *in vivo*. However, the experiment should be redone using stable *LINC1* silencing cell lines to determine if there is long-term effect on cellular growth.

5 Conclusion and outlook

In conclusion our findings suggest that silencing of *LINC1* resulted in less cancerous behavior in all four independent colorectal cancer cell lines HCT116, HRT-18, SW480 and DLD1, suggesting that it might serve as oncogene.

Knock down of *LINC1* impacts anchorage independent growth and colony formation ability as well as cell proliferation potentially through mediating increased apoptotic activity in CRC cell lines. It also led to G1 phase arrest in two cell lines and seems to influence cell migration.

Furthermore *LINC1* has an impact on stem cell like properties by inducing a decrease in tumor sphere formation. However we could not confirm our *in vitro* results in an *in vivo* mouse model. Since *LINC1* is a quite unknown lncRNA not much information about the biochemical mechanisms or biological behavior is provided. Further prospective studies and clinical trials are needed to proof the role of *LINC1* as a prognostic marker and furthermore evaluate if *LINC1* silencing carries therapeutic value in patients with CRC.

6 References

1. Siegel RL, Miller KD, Jemal A. Cancer statistics, 2016. *CA: a cancer journal for clinicians*. 2016;66:7-30.
2. Winawer SJ, Fletcher RH, Miller L, Godlee F, Stolar MH, Mulrow CD, et al. Colorectal cancer screening: Clinical guidelines and rationale. *Gastroenterology*. 1997;112:594-642.
3. Eaden JA, Abrams KR, Mayberry JF. The risk of colorectal cancer in ulcerative colitis: a meta-analysis. *Gut*. 2001;48:526-35.
4. Johns LE, Houlston RS. A systematic review and meta-analysis of familial colorectal cancer risk. *The American journal of gastroenterology*. 2001;96:2992-3003.
5. Robertson DJ. ABC of Colorectal Cancer. *Gastroenterology*. 2012;143:868-9.
6. Martinez-Useros J, Garcia-Foncillas J. Obesity and colorectal cancer: molecular features of adipose tissue. *Journal of translational medicine*. 2016;14:21.
7. Botteri E, Iodice S, Bagnardi V, Raimondi S, Lowenfels AB, Maisonneuve P. Smoking and colorectal cancer: a meta-analysis. *Jama*. 2008;300:2765-78.
8. Cross AJ, Boca S, Freedman ND, Caporaso NE, Huang WY, Sinha R, et al. Metabolites of tobacco smoking and colorectal cancer risk. *Carcinogenesis*. 2014;35:1516-22.
9. Fearon ER, Vogelstein B. A genetic model for colorectal tumorigenesis. *Cell*. 1990;61:759-67.
10. Smith G, Carey FA, Beattie J, Wilkie MJ, Lightfoot TJ, Coxhead J, et al. Mutations in APC, Kirsten-ras, and p53--alternative genetic pathways to colorectal cancer. *Proceedings of the National Academy of Sciences of the United States of America*. 2002;99:9433-8.
11. Weisenberger DJ, Siegmund KD, Campan M, Young J, Long TI, Faasse MA, et al. CpG island methylator phenotype underlies sporadic microsatellite instability and is tightly associated with BRAF mutation in colorectal cancer. *Nature genetics*. 2006;38:787-93.
12. East JE, Saunders BP, Jass JR. Sporadic and syndromic hyperplastic polyps and serrated adenomas of the colon: classification, molecular genetics, natural history, and clinical management. *Gastroenterology clinics of North America*. 2008;37:25-46, v.

13. Cunningham D, Atkin W, Lenz H-J, Lynch HT, Minsky B, Nordlinger B, et al. Colorectal cancer. *The Lancet*. 2010;375:1030-47.
14. Kerr D. Clinical development of gene therapy for colorectal cancer. *Nat Rev Cancer*. 2003;3:615-22.
15. Etienne MC, Chazal M, Laurent-Puig P, Magne N, Rosty C, Formento JL, et al. Prognostic value of tumoral thymidylate synthase and p53 in metastatic colorectal cancer patients receiving fluorouracil-based chemotherapy: phenotypic and genotypic analyses. *Journal of clinical oncology : official journal of the American Society of Clinical Oncology*. 2002;20:2832-43.
16. Heidelberger C, Chaudhuri NK, Danneberg P, Mooren D, Griesbach L, Duschinsky R, et al. Fluorinated pyrimidines, a new class of tumour-inhibitory compounds. *Nature*. 1957;179:663-6.
17. Peters GJ, van Groeningen CJ. Clinical relevance of biochemical modulation of 5-fluorouracil. *Annals of oncology : official journal of the European Society for Medical Oncology*. 1991;2:469-80.
18. Longley DB, Harkin DP, Johnston PG. 5-fluorouracil: mechanisms of action and clinical strategies. *Nat Rev Cancer*. 2003;3:330-8.
19. Douillard JY, Cunningham D, Roth AD, Navarro M, James RD, Karasek P, et al. Irinotecan combined with fluorouracil compared with fluorouracil alone as first-line treatment for metastatic colorectal cancer: a multicentre randomised trial. *Lancet*. 2000;355:1041-7.
20. Giacchetti S, Perpoint B, Zidani R, Le Bail N, Faggiuolo R, Focan C, et al. Phase III multicenter randomized trial of oxaliplatin added to chronomodulated fluorouracil-leucovorin as first-line treatment of metastatic colorectal cancer. *Journal of clinical oncology : official journal of the American Society of Clinical Oncology*. 2000;18:136-47.
21. Douillard JY, Sobrero A, Carnaghi C, Comella P, Diaz-Rubio E, Santoro A, et al. Metastatic colorectal cancer: integrating irinotecan into combination and sequential chemotherapy. *Annals of oncology : official journal of the European Society for Medical Oncology*. 2003;14 Suppl 2:ii7-12.
22. Cunningham D, Humblet Y, Siena S, Khayat D, Bleiberg H, Santoro A, et al. Cetuximab monotherapy and cetuximab plus irinotecan in irinotecan-refractory metastatic colorectal cancer. *The New England journal of medicine*. 2004;351:337-45.

23. Hurwitz H, Fehrenbacher L, Novotny W, Cartwright T, Hainsworth J, Heim W, et al. Bevacizumab plus irinotecan, fluorouracil, and leucovorin for metastatic colorectal cancer. *The New England journal of medicine*. 2004;350:2335-42.
24. Messa C, Russo F, Gabriella Caruso M, Di Leo A. EGF, TGF- α , and EGF-R in Human Colorectal Adenocarcinoma. *Acta Oncologica*. 1998;37:285-9.
25. Porębska I, Harłózińska A, Bojarowski T. Expression of the Tyrosine Kinase Activity Growth Factor Receptors (EGFR, ERB B2, ERB B3) in Colorectal Adenocarcinomas and Adenomas. *Tumor Biology*. 2000;21:105-15.
26. Salomon DS, Brandt R, Ciardiello F, Normanno N. Epidermal growth factor-related peptides and their receptors in human malignancies. *Critical reviews in oncology/hematology*. 1995;19:183-232.
27. Ciardiello F, Tortora G. A novel approach in the treatment of cancer: targeting the epidermal growth factor receptor. *Clinical cancer research : an official journal of the American Association for Cancer Research*. 2001;7:2958-70.
28. Klapper LN, Kirschbaum MH, Sela M, Yarden Y. Biochemical and clinical implications of the ErbB/HER signaling network of growth factor receptors. *Advances in cancer research*. 2000;77:25-79.
29. Misale S, Yaeger R, Hobor S, Scala E, Janakiraman M, Liska D, et al. Emergence of KRAS mutations and acquired resistance to anti-EGFR therapy in colorectal cancer. *Nature*. 2012;486:532-6.
30. Moroni M, Veronese S, Benvenuti S, Marrapese G, Sartore-Bianchi A, Di Nicolantonio F, et al. Gene copy number for epidermal growth factor receptor (EGFR) and clinical response to antiEGFR treatment in colorectal cancer: a cohort study. *The Lancet Oncology*. 2005;6:279-86.
31. Personeni N, Fieuws S, Piessevaux H, De Hertogh G, De Schutter J, Biesmans B, et al. Clinical usefulness of EGFR gene copy number as a predictive marker in colorectal cancer patients treated with cetuximab: a fluorescent in situ hybridization study. *Clinical cancer research : an official journal of the American Association for Cancer Research*. 2008;14:5869-76.
32. An integrated encyclopedia of DNA elements in the human genome. *Nature*. 2012;489:57-74.
33. Carninci P, Kasukawa T, Katayama S, Gough J, Frith MC, Maeda N, et al. The transcriptional landscape of the mammalian genome. *Science*. 2005;309:1559-63.

34. Birney E, Stamatoyannopoulos JA, Dutta A, Guigo R, Gingeras TR, Margulies EH, et al. Identification and analysis of functional elements in 1% of the human genome by the ENCODE pilot project. *Nature*. 2007;447:799-816.
35. Meseure D, Drak Alsibai K, Nicolas A, Bieche I, Morillon A. Long Noncoding RNAs as New Architects in Cancer Epigenetics, Prognostic Biomarkers, and Potential Therapeutic Targets. *BioMed research international*. 2015;2015:320214.
36. Mercer TR, Dinger ME, Mattick JS. Long non-coding RNAs: insights into functions. *Nature reviews Genetics*. 2009;10:155-9.
37. Liu Q, Huang J, Zhou N, Zhang Z, Zhang A, Lu Z, et al. LncRNA loc285194 is a p53-regulated tumor suppressor. *Nucleic acids research*. 2013;41:4976-87.
38. Gupta RA, Shah N, Wang KC, Kim J, Horlings HM, Wong DJ, et al. Long non-coding RNA HOTAIR reprograms chromatin state to promote cancer metastasis. *Nature*. 2010;464:1071-6.
39. Pibouin L, Villaudy J, Ferbus D, Muleris M, Prosperi MT, Remvikos Y, et al. Cloning of the mRNA of overexpression in colon carcinoma-1: a sequence overexpressed in a subset of colon carcinomas. *Cancer genetics and cytogenetics*. 2002;133:55-60.
40. Aiello A, Bacci L, Re A, Ripoli C, Pierconti F, Pinto F, et al. MALAT1 and HOTAIR Long Non-Coding RNAs Play Opposite Role in Estrogen-Mediated Transcriptional Regulation in Prostate Cancer Cells. *Scientific reports*. 2016;6:38414.
41. Yan J, Dang Y, Liu S, Zhang Y, Zhang G. LncRNA HOTAIR promotes cisplatin resistance in gastric cancer by targeting miR-126 to activate the PI3K/AKT/MRP1 genes. *Tumour biology : the journal of the International Society for Oncodevelopmental Biology and Medicine*. 2016.
42. Sun J, Chu H, Ji J, Huo G, Song Q, Zhang X. Long non-coding RNA HOTAIR modulates HLA-G expression by absorbing miR-148a in human cervical cancer. *International journal of oncology*. 2016;49:943-52.
43. Milevskiy MJ, Al-Ejeh F, Saunus JM, Northwood KS, Bailey PJ, Betts JA, et al. Long-range regulators of the lncRNA HOTAIR enhance its prognostic potential in breast cancer. *Human molecular genetics*. 2016;25:3269-83.
44. Kogo R, Shimamura T, Mimori K, Kawahara K, Imoto S, Sudo T, et al. Long noncoding RNA HOTAIR regulates polycomb-dependent chromatin modification and is associated with poor prognosis in colorectal cancers. *Cancer research*. 2011;71:6320-6.

45. Dou J, Ni Y, He X, Wu D, Li M, Wu S, et al. Decreasing lncRNA HOTAIR expression inhibits human colorectal cancer stem cells. *American journal of translational research*. 2016;8:98-108.
46. Svoboda M, Slysokova J, Schneiderova M, Makovicky P, Bielik L, Levy M, et al. HOTAIR long non-coding RNA is a negative prognostic factor not only in primary tumors, but also in the blood of colorectal cancer patients. *Carcinogenesis*. 2014;35:1510-5.
47. Younger ST, Rinn JL. 'Lnc'-ing enhancers to MYC regulation. *Cell research*. 2014;24:643-4.
48. Zhang E, Han L, Yin D, He X, Hong L, Si X, et al. H3K27 acetylation activated-long non-coding RNA CCAT1 affects cell proliferation and migration by regulating SPRY4 and HOXB13 expression in esophageal squamous cell carcinoma. *Nucleic acids research*. 2017;45:3086-101.
49. Guo X, Hua Y. CCAT1: an oncogenic long noncoding RNA in human cancers. *Journal of cancer research and clinical oncology*. 2017;143:555-62.
50. Nissan A, Stojadinovic A, Mitrani-Rosenbaum S, Halle D, Grinbaum R, Roistacher M, et al. Colon cancer associated transcript-1: a novel RNA expressed in malignant and pre-malignant human tissues. *International journal of cancer*. 2012;130:1598-606.
51. Zhao W, Song M, Zhang J, Kuerban M, Wang H. Combined identification of long non-coding RNA CCAT1 and HOTAIR in serum as an effective screening for colorectal carcinoma. *International journal of clinical and experimental pathology*. 2015;8:14131-40.
52. He X, Tan X, Wang X, Jin H, Liu L, Ma L, et al. C-Myc-activated long noncoding RNA CCAT1 promotes colon cancer cell proliferation and invasion. *Tumour biology : the journal of the International Society for Oncodevelopmental Biology and Medicine*. 2014;35:12181-8.
53. Ye Z, Zhou M, Tian B, Wu B, Li J. Expression of lncRNA-CCAT1, E-cadherin and N-cadherin in colorectal cancer and its clinical significance. *International journal of clinical and experimental medicine*. 2015;8:3707-15.
54. Alaiyan B, Ilyayev N, Stojadinovic A, Izadjoo M, Roistacher M, Pavlov V, et al. Differential expression of colon cancer associated transcript1 (CCAT1) along the colonic adenoma-carcinoma sequence. *BMC cancer*. 2013;13:196.

55. Wang Y, Xue D, Li Y, Pan X, Zhang X, Kuang B, et al. The Long Noncoding RNA MALAT-1 is A Novel Biomarker in Various Cancers: A Meta-analysis Based on the GEO Database and Literature. *Journal of Cancer*. 2016;7:991-1001.
56. Han T, Jiao F, Hu H, Yuan C, Wang L, Jin ZL, et al. EZH2 promotes cell migration and invasion but not alters cell proliferation by suppressing E-cadherin, partly through association with MALAT-1 in pancreatic cancer. *Oncotarget*. 2016;7:11194-207.
57. Tang R, Jiang M, Liang L, Xiong D, Dang Y, Chen G. Long Noncoding RNA MALAT-1 Can Predict Poor Prognosis: A Meta-Analysis. *Medical science monitor : international medical journal of experimental and clinical research*. 2016;22:302-9.
58. Yang MH, Hu ZY, Xu C, Xie LY, Wang XY, Chen SY, et al. MALAT1 promotes colorectal cancer cell proliferation/migration/invasion via PRKA kinase anchor protein 9. *Biochimica et biophysica acta*. 2015;1852:166-74.
59. Liu FT, Zhu PQ, Luo HL, Zhang Y, Hao TF, Xia GF, et al. Long noncoding RNA ANRIL: a potential novel prognostic marker in cancer: a meta-analysis. *Minerva medica*. 2016;107:77-83.
60. Zheng HT, Shi DB, Wang YW, Li XX, Xu Y, Tripathi P, et al. High expression of lncRNA MALAT1 suggests a biomarker of poor prognosis in colorectal cancer. *International journal of clinical and experimental pathology*. 2014;7:3174-81.
61. Xu C, Yang M, Tian J, Wang X, Li Z. MALAT-1: a long non-coding RNA and its important 3' end functional motif in colorectal cancer metastasis. *International journal of oncology*. 2011;39:169-75.
62. Cui H, Onyango P, Brandenburg S, Wu Y, Hsieh CL, Feinberg AP. Loss of imprinting in colorectal cancer linked to hypomethylation of H19 and IGF2. *Cancer research*. 2002;62:6442-6.
63. Liu FT, Pan H, Xia GF, Qiu C, Zhu ZM. Prognostic and clinicopathological significance of long noncoding RNA H19 overexpression in human solid tumors: evidence from a meta-analysis. *Oncotarget*. 2016;7:83177-86.
64. Liu X, Jiao T, Wang Y, Su W, Tang Z, Han C. Long non-coding RNA GAS5 acts as a molecular sponge to regulate miR-23a in gastric cancer. *Minerva medica*. 2016.
65. Tsang WP, Ng EK, Ng SS, Jin H, Yu J, Sung JJ, et al. Oncofetal H19-derived miR-675 regulates tumor suppressor RB in human colorectal cancer. *Carcinogenesis*. 2010;31:350-8.

66. Huarte M, Guttman M, Feldser D, Garber M, Koziol MJ, Kenzelmann-Broz D, et al. A large intergenic noncoding RNA induced by p53 mediates global gene repression in the p53 response. *Cell*. 2010;142:409-19.
67. Guo XB, Hua Z, Li C, Peng LP, Wang JS, Wang B, et al. Biological significance of long non-coding RNA FTX expression in human colorectal cancer. *International journal of clinical and experimental medicine*. 2015;8:15591-600.
68. Tang SS, Zheng BY, Xiong XD. LincRNA-p21: Implications in Human Diseases. *International Journal of Molecular Sciences*. 2015;16:18732-40.
69. Yang N, Fu Y, Zhang H, Sima H, Zhu N, Yang G. LincRNA-p21 activates endoplasmic reticulum stress and inhibits hepatocellular carcinoma. *Oncotarget*. 2015;6:28151-63.
70. Zhu L, Liu J, Ma S, Zhang S. Long Noncoding RNA MALAT-1 Can Predict Metastasis and a Poor Prognosis: a Meta-Analysis. *Pathology oncology research : POR*. 2015;21:1259-64.
71. Yang C, Li Z, Li Y, Xu R, Wang Y, Tian Y, et al. Long non-coding RNA NEAT1 overexpression is associated with poor prognosis in cancer patients: a systematic review and meta-analysis. *Oncotarget*. 2017;8:2672-80.
72. Huang G, Zhu H, Shi Y, Wu W, Cai H, Chen X. cir-ITCH plays an inhibitory role in colorectal cancer by regulating the Wnt/beta-catenin pathway. *PLoS ONE*. 2015;10:e0131225.
73. Johnsson P, Lipovich L, Grandér D, Morris KV. Evolutionary conservation of long noncoding RNAs; sequence, structure, function. *Biochimica et biophysica acta*. 2014;1840:1063-71.
74. Khalil AM, Guttman M, Huarte M, Garber M, Raj A, Rivea Morales D, et al. Many human large intergenic noncoding RNAs associate with chromatin-modifying complexes and affect gene expression. *Proceedings of the National Academy of Sciences of the United States of America*. 2009;106:11667-72.
75. Margueron R, Reinberg D. The Polycomb complex PRC2 and its mark in life. *Nature*. 2011;469:343-9.
76. Guttman M, Rinn JL. Modular regulatory principles of large non-coding RNAs. *Nature*. 2012;482:339-46.
77. Wutz A. Gene silencing in X-chromosome inactivation: advances in understanding facultative heterochromatin formation. *Nature reviews Genetics*. 2011;12:542-53.

78. Schmittgen TD, Livak KJ. Analyzing real-time PCR data by the comparative C(T) method. *Nature protocols*. 2008;3:1101-8.
79. Nagano T, Fraser P. No-nonsense functions for long noncoding RNAs. *Cell*. 2011;145:178-81.
80. Kung JT, Colognori D, Lee JT. Long noncoding RNAs: past, present, and future. *Genetics*. 2013;193:651-69.
81. Gibb EA, Brown CJ, Lam WL. The functional role of long non-coding RNA in human carcinomas. *Molecular cancer*. 2011;10:38.
82. Ji Q, Zhang L, Liu X, Zhou L, Wang W, Han Z, et al. Long non-coding RNA MALAT1 promotes tumour growth and metastasis in colorectal cancer through binding to SFPQ and releasing oncogene PTBP2 from SFPQ/PTBP2 complex. *British journal of cancer*. 2014;111:736-48.
83. Derrien T, Johnson R, Bussotti G, Tanzer A, Djebali S, Tilgner H, et al. The GENCODE v7 catalog of human long noncoding RNAs: analysis of their gene structure, evolution, and expression. *Genome research*. 2012;22:1775-89.
84. Kaelin WG, Jr. Molecular biology. Use and abuse of RNAi to study mammalian gene function. *Science*. 2012;337:421-2.
85. Agrawal N, Dasaradhi PV, Mohmmmed A, Malhotra P, Bhatnagar RK, Mukherjee SK. RNA interference: biology, mechanism, and applications. *Microbiology and molecular biology reviews : MMBR*. 2003;67:657-85.
86. Holen T, Amarzguioui M, Wiiger MT, Babaie E, Prydz H. Positional effects of short interfering RNAs targeting the human coagulation trigger Tissue Factor. *Nucleic acids research*. 2002;30:1757-66.
87. Franken NA, Rodermond HM, Stap J, Haveman J, van Bree C. Clonogenic assay of cells in vitro. *Nature protocols*. 2006;1:2315-9.
88. Borowicz S, Van Scoyk M, Avasarala S, Karuppusamy Rathinam MK, Tauler J, Bikkavilli RK, et al. The soft agar colony formation assay. *Journal of visualized experiments : JoVE*. 2014:e51998.
89. Su J, Zhang E, Han L, Yin D, Liu Z, He X, et al. Long noncoding RNA BLACAT1 indicates a poor prognosis of colorectal cancer and affects cell proliferation by epigenetically silencing of p15. *Cell Death & Disease*. 2017;8:e2665.
90. Xue L, Zhu Z, Wang Z, Li H, Zhang P, Wang Z, et al. Knockdown of prostaglandin reductase 1 (PTGR1) suppresses prostate cancer cell proliferation by inducing cell cycle arrest and apoptosis. *Bioscience trends*. 2016;10:133-9.

91. Du X, Lin LI, Zhang L, Jiang JIE. microRNA-195 inhibits the proliferation, migration and invasion of cervical cancer cells via the inhibition of CCND2 and MYB expression. *Oncology Letters*. 2015;10:2639-43.
92. Sherr CJ. Cancer cell cycles. *Science*. 1996;274:1672-7.
93. Ding J, Xie M, Lian Y, Zhu Y, Peng P, Wang J, et al. Long noncoding RNA HOXA-AS2 represses P21 and KLF2 expression transcription by binding with EZH2, LSD1 in colorectal cancer. *Oncogenesis*. 2017;6:e288.
94. Vogel C, Marcotte EM. Insights into the regulation of protein abundance from proteomic and transcriptomic analyses. *Nature reviews Genetics*. 2012;13:227-32.
95. Maier T, Guell M, Serrano L. Correlation of mRNA and protein in complex biological samples. *FEBS letters*. 2009;583:3966-73.
96. Peiris-Pagès M, Martinez-Outschoorn UE, Pestell RG, Sotgia F, Lisanti MP. Cancer stem cell metabolism. *Breast Cancer Research : BCR*. 2016;18:55.
97. Liang CC, Park AY, Guan JL. In vitro scratch assay: a convenient and inexpensive method for analysis of cell migration in vitro. *Nature protocols*. 2007;2:329-33.
98. Yu T, Shan TD, Li JY, Huang CZ, Wang SY, Ouyang H, et al. Knockdown of linc-UFC1 suppresses proliferation and induces apoptosis of colorectal cancer. *Cell Death & Disease*. 2016;7:e2228.